


Defect Conformal Field Theory from Sachdev-Ye-Kitaev Interactions

Yang Ge  and Shao-Kai Jian *

Department of Physics and Engineering Physics, Tulane University, New Orleans, Louisiana 70118, USA

(Dated: December 30, 2024)

The coupling between defects and extended critical degrees of freedom gives rise to the intriguing theory known as defect conformal field theory (dCFT). In this work, we introduce a novel family of boundary and interface CFTs by coupling N Majorana chains with SYK $_q$ interactions at the defect. Our analysis reveals that the interaction with $q = 2$ constitutes a new marginal defect. Employing a versatile saddle-point method, we compute unique entanglement characterizations, including the g function and effective central charge, of the defect CFT. Furthermore, we analytically evaluate the transmission coefficient using CFT techniques. Surprisingly, the transmission coefficient deviates from the universal relation with the effective central charge across the defect at the large N limit, suggesting that our defect CFT extends beyond all known examples of Gaussian defect CFT.

Introduction—Understanding the defect or boundary conformal field theory (CFT) holds significant implications across various domains of theoretical physics [1–3]. In condensed matter physics, defect CFT (dCFT) provides a powerful framework for deciphering critical behaviors of complex materials characterized by boundaries, interfaces, and defects, all common in the real world. In particular, boundary phenomena host the most interesting physics in symmetry-protected topological phases [4, 5]. Within the framework of string theory, dCFT naturally emerges in the study of D-branes [6, 7], offering insights on topics including brane intersections and holographic correspondences [8–10] between gravitational theories and boundary CFTs [11, 12].

Transmission and reflection are important characterizations of interfaces in CFTs [13, 14]. Interactions can render defects relevant or irrelevant, leading to asymptotic behaviors where defects become completely reflective or transmitting. In 2D free massless fermion theories, it was discovered that defects can be marginal, resulting in partial transmission and reflection [14–19]. Beyond free dCFTs, non-Gaussian defects are only understood on a case-by-case basis. Two special cases are the totally reflective factorizing defect and the perfectly transmitting topological defect in rational CFTs [20, 21]. Defects other than total transmitters or reflectors in two dimensions include the symmetry breaking defect via a coset construction [22], permutationlike boundary conditions in Wess-Zumino-Witten and coset models [23, 24], defects in the tricritical Ising model [25], as well as in minimal models with rational products [14] or random defects [26]. Higher-dimensional cases include defects in the 3D Ising model [27], $O(N)$ model [28–33], Super-Yang-Mills theories [34–37], the AdS/dCFT construction [11, 12], as well as the Kondo model [38].

Entanglement emerges as a useful characterization of many-body wave functions [39–42]. Many-body entanglement can be quantified with the celebrated Rényi entropy [43]: given a many-body wave function $|\Psi\rangle$ and a bipartition $A \cup B$, the Rényi entropy is $S_n(A) = \frac{1}{1-n} \log \text{Tr}[\rho_A^n]$, with $\rho_A = \text{Tr}_B[\rho]$ being the reduced density matrix on A . While the entanglement entropy in a CFT is closely related to its central charge [44–47], it can be altered by defects. In this context, the boundary entropy, or g function [48], universally

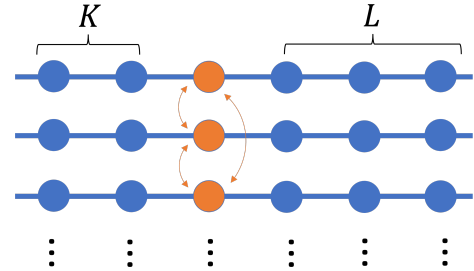


FIG. 1. Illustration of the lattice model. The dots denote each site of the Majorana chain. There are N free Majorana chains, that are coupled via SYK interactions at the orange site, dubbed the SYK site. Open boundary condition is assumed and the number of sites to the left (right) of the SYK site is K (L).

characterizes the ground state degeneracy in the presence of boundaries or defects. More explicitly, boundary conditions contribute to the free energy by a constant independent of its system size L when L is large. Additionally, for marginal defects in free fermion CFTs, the Rényi entropy across the defect is captured by an effective central charge, which exhibits a universal function of the transmission coefficient [49–57].

The Sachdev-Ye-Kitaev (SYK) model [58–61], a 0+1D quantum model, presents a unique and solvable candidate for defects beyond all known examples. Initially introduced as a solvable toy model, with intriguing properties akin to black holes, the SYK model has found solvable generalizations in various fields, including non-Fermi liquid behavior [62–67], thermalization [68–74], and non-Hermitian physics [75–79]. The interplay between the SYK model and CFTs has been studied in the context of black hole evaporation [80–83]. However, the joint system, where SYK acts as a defect [84–86], remains relatively unexplored. Key questions include constructing a dCFT from the SYK model and identifying unique characterizations of such a dCFT.

In this Letter, we build boundary and defect CFTs by coupling N Majorana chains with SYK $_q$ -type interactions at the defect, illustrated in Fig. 1. We show that the interaction is marginal for $q = 2$, and irrelevant for $q > 2$. For $q = 2$, the analytical conformal solution gives a tunable transmission coefficient. We develop a saddle-point method to investigate

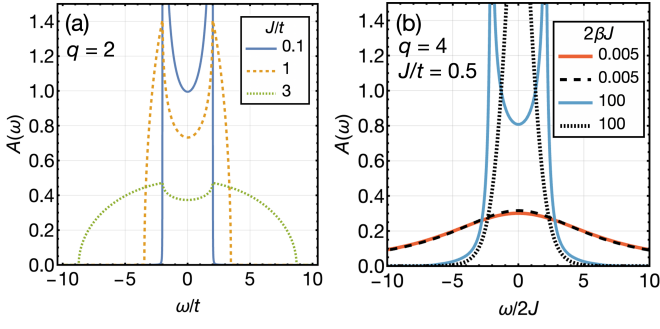


FIG. 2. Local spectral functions at the SYK_q site on infinite chains. (a) The SYK₂-site spectral function at various J/t , independent of temperature. (b) Temperature evolution of the spectral function at the SYK₄ site with $J/t = 0.5$. Dashed curves show the spectral functions of the bare SYK₄ model. Deviation from the SYK₄ fixed point at low temperature near zero frequency shows the irrelevance. The spectral function flow is settled at $2\beta J \sim 0.2$.

the Rényi entropy of various bipartitions in the joint system. In an islandlike bipartition, the g function is shown to be 1. Finally, we compute the Rényi entropy across the SYK defect and extract a continuous effective central charge on the SYK interaction strength. Unlike known Gaussian dCFTs, the universal relation between the effective central charge and the transmission breaks down for the SYK₂ defect [54], owing to the non-Gaussianity induced by the random coupling in SYK.

Model—We consider the Hamiltonian $H = H_{\text{CFT}} + H_1$, where $H_{\text{CFT}} = -i2t \sum_{jr} \psi_{j,r} \psi_{j,r+1}$ consists of $j=1, \dots, N$ decoupled Majorana chains with nearest-neighbor hoppings of amplitude t between sites r and $r+1$, while $H_1 = i^{q/2} \sum_{j_1, \dots, j_q} J_{j_1, \dots, j_q} \psi_{j_1,0} \dots \psi_{j_q,0}$ couples the chains by the SYK_q interaction of strength J at the site $r=0$, dubbed the SYK site. Thus, each site has N Majorana fermions so that $\{\psi_{j,r}, \psi_{j',r'}\} = \delta_{j,j'} \delta_{r,r'}$. The interaction strength J_{j_1, \dots, j_q} is a Gaussian variable with mean zero and variance $\overline{J_{j_1, \dots, j_q} J_{j'_1, \dots, j'_q}} = \delta_{j_1, j'_1} \dots \delta_{j_q, j'_q} \frac{2^{q-1} J^2 (q-1)!}{N^{q-1}}$. Figure 1 shows the schematic.

We use the (G, Σ) -action at the SYK site to solve the model [60, 71, 87, 88], with $G(\tau) = \frac{1}{N} \sum_j \langle \psi_{j,0}(\tau) \psi_{j,0}(0) \rangle$, and Σ being the corresponding self-energy [89]. Here the angle bracket denotes both quantum and disorder averages, and τ is imaginary time. In the large- N limit, the Schwinger-Dyson equations are

$$\begin{aligned} G^{-1}(i\omega_n) &= -i\omega_n - \Sigma(i\omega_n) - tR_K\left(\frac{-i\omega_n}{2t}\right) - tR_L\left(\frac{-i\omega_n}{2t}\right), \\ \Sigma(\tau) &= J^2 [2G(\tau)]^{q-1}, \end{aligned} \quad (1)$$

where $G(i\omega_n) \equiv \int d\tau G(\tau) e^{i\omega_n \tau}$ with the Matsubara frequencies $\omega_n \equiv (2n+1)\pi/\beta$ at the inverse temperature β . Coupling to the rest of the chains results in the self-energy terms of the form $R_L(x) \equiv \frac{U_{L-1}(x)}{U_L(x)}$, where U is the Chebyshev polynomial of the second kind [90, 91].

A simple scaling analysis reveals that the SYK interaction is marginal for $q=2$ and irrelevant for $q>2$, since the scaling dimension of J is $1 - \frac{q}{2}$. This is confirmed by exactly solv-

ing the model in the thermodynamic limit, $K, L \rightarrow \infty$, using $\lim_{L \rightarrow \infty} R_L(x) = x - \sqrt{x^2 - 1}$. The local spectral function at the SYK site, $A(\omega) \equiv 2G''(\omega - i\eta)$ is used to expand G and express Σ [89, 92]. Thus, $A(\omega)$ is obtained exactly and plotted in Fig. 2. For $q=2$, the interaction is indeed marginal and $A(\omega)$ temperature independent. Across all J/t in Fig. 2(a), it features two peaks coming from the band edges of the Majorana chain, and a semicircle coming from the SYK₂ site. On the other hand, $A(\omega)$ is temperature dependent when $q>2$. Figure 2(b) shows the example of the $q=4$ case along with that of a decoupled SYK₄ site. At low temperature and near zero frequency, $A(\omega)$ flows away from the SYK fixed point, demonstrating its irrelevance. Consequently, we will focus on $q=2$ from now on.

In the SYK₂ case, the full Green's function on the chains takes a simple analytic form in the thermodynamic limit [89], which can be derived from the Dyson equation that consists of the Green's function of the free Majorana chain G_0 and the self energy Σ at the SYK site, $G(r, r'; i\omega_n) = G_0(r, r'; i\omega_n) + G_0(r, 0; i\omega_n) \Sigma(i\omega_n) G(0, r'; i\omega_n)$. To further study the low-energy physics we focus on the left- and right-propagating chiral modes at the Fermi surface, $k_F = 0$ and π , with the lattice constant set to 1. They are $\psi_{L,R}(x) \sim \int_{k \sim 0, \pi} e^{-ikx} \psi(k) dk$. Together they form a Dirac spinor $\Psi = (\psi_L, \psi_R)^T$. After coarse graining [89], the effective action for the SYK₂ model becomes a dCFT:

$$\mathcal{L}_{\text{dCFT}} = \sum_j \Psi_j^\dagger (\partial_\tau - it\partial_x \sigma^z) \Psi_j + \sum_{jl} i\delta(x) \tilde{J}_{jl} \Psi_j^\dagger P \Psi_l, \quad (2)$$

where $\tilde{J} \equiv J/t$ and $P = \frac{1}{2} \begin{pmatrix} 1 & 1 \\ 1 & -1 \end{pmatrix}$. The continuum Green's function can be solved explicitly to reveal its conformal nature [89]. By conformal symmetry, higher-order correlators recursively reduce to the single-particle Green's function [17].

Transmission and reflection—A dCFT is characterized by its transmission and reflection coefficients, \mathcal{T} and $\mathcal{R} = 1 - \mathcal{T}$, across the defect [14, 17]. They are the corresponding probabilities in single-particle free field theories. For a conformal defect at $x=0$, the transmission coefficient is defined by the holomorphic and antiholomorphic components of the stress-energy tensor, T and \bar{T} , at two sides of the defect [14],

$$\mathcal{T} \equiv \frac{\langle T(x)T(-x) + \bar{T}(x)\bar{T}(-x) \rangle}{\langle [T(x) + \bar{T}(-x)][\bar{T}(x) + T(-x)] \rangle}. \quad (3)$$

For the low energy CFT of the SYK₂ defect [89]

$$\mathcal{T} = \frac{2}{3 + \tilde{J}^2 - \sqrt{1 + 2\tilde{J}^2}}. \quad (4)$$

In general, coarse graining need not produce a simple relation between the lattice parameters at UV and continuum parameters at IR. Still, solutions to both the lattice and the continuum model (2) produce the same transmission coefficient [89], with $\tilde{J}^2 \rightarrow J^2/(t^2 \cos^2 k)$. Thus, $\tilde{J} = J/t$ holds at long wavelengths for all J/t . At small J , $1 - \mathcal{T} \sim \tilde{J}^4/4$. Our defect formally corresponds to the Dirichlet boundary condition in

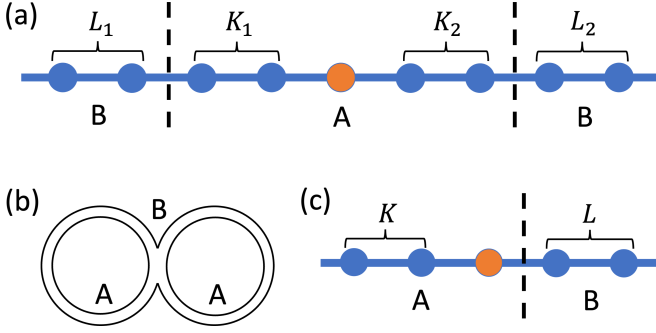


FIG. 3. (a) Generic bipartition of 1+1D open chains. For simplicity, a single chain is plotted, which nevertheless should be understood as N chains. (b) The imaginary time contour for the second Rényi entropy. The fermionic field in a closed contour satisfies the conventional antiperiodic boundary condition associated with the fermionic Matsubara frequency. Region B has the twisted boundary condition threading the two replicas. (c) Setup for the interface CFT induced at the SYK site, where $L_1 = K_2 = 0$.

the Ising CFT, that is $|D, \phi\rangle$ with $\phi = \frac{1}{2} \arcsin \sqrt{\mathcal{T}}$ [16, 53]. As for SYK $_q$ defects with $q > 2$, $\mathcal{T} = 1$ due to their irrelevance.

Rényi entropy—Sitting between two 1+1D CFTs, the SYK defect encodes the entanglement across it in the conformal data of its dCFT [49, 53, 54]. Using the replica trick and the large- N analysis, we present a method [73, 82, 93] to conveniently extract the Rényi entanglement entropy for an arbitrary bipartition as depicted in Fig. 3(a). Below, the second Rényi entropy is computed as an example and later used to obtain the g function as well as the effective central charge.

The second Rényi entropy of region A is given by partial traces over the reduced density matrix,

$$S_2 = -\log \text{Tr}_A [(\text{Tr}_B \rho)^2] = -\log [Z_{(2)}/Z^2]. \quad (5)$$

The replica trick conducts the partial trace with different imaginary-time boundary conditions in regions A and B [44, 73, 82]. Here $Z_{(2)}$ denotes a two-replica path integral with a twisted boundary condition in region B , while Z is the path integral corresponding to the thermal density matrix $\rho \equiv e^{-\beta H}/Z$. Boundary conditions of the replica fields differ between regions A and B : in region A , $\psi^{(1)}(\beta) = -\psi^{(1)}(0)$, $\psi^{(2)}(\beta) = -\psi^{(2)}(0)$, whereas in region B , $\psi^{(1)}(\beta) = \psi^{(2)}(0)$, $\psi^{(2)}(\beta) = -\psi^{(1)}(0)$. The superscripts 1 and 2 denote the two replicas. This imaginary time contour for $Z_{(2)}$ is depicted in Fig. 3(b). We join the two replicas to span $\tau \in (0, 2\beta)$, so that fields can be expanded in Matsubara frequencies $\omega_n^{(1)} = \omega_n^{(2)} = (2n+1)\pi/\beta$ in region A , and $\Omega_n = (2n+1)\pi/2\beta$ in region B . Namely, in region A , $\psi(\tau) = \frac{1}{\sqrt{\beta}} \sum_n \psi(i\omega_n^{(1)}) e^{-i\omega_n^{(1)}\tau} \Theta(\beta - \tau) + \frac{1}{\sqrt{\beta}} \sum_n \psi(i\omega_n^{(2)}) e^{-i\omega_n^{(2)}\tau} \Theta(\tau - \beta)$, whereas in region B , $\psi(\tau) = \frac{1}{\sqrt{2\beta}} \sum_n \psi(i\Omega_n) e^{-i\Omega_n\tau}$.

At large N , we solve for the saddle-point Green's function $G_{(2)}$ at the SYK site, and then substitute it into the twisted action to compute $Z_{(2)}$ [89]. The time-translation symmetry

is broken in $Z_{(2)}$ due to the twist operator σ at the partition interface, which is defined below. The solution is

$$\begin{aligned} G_{(2)}^{-1}(i\omega_m^{(a)}, i\omega_n^{(b)}) &= -i\omega_n^{(a)} \delta_{ab} \delta_{mn} - \Sigma_{(2)}(i\omega_m^{(a)}, i\omega_n^{(b)}) \\ &\quad - t(\mathbf{D}_{K_1, L_1})_{mn}^{ab} - t(\mathbf{D}_{K_2, L_2})_{mn}^{ab}, \\ \Sigma_{(2)}(\tau_1, \tau_2) &= J^2 [2G_{(2)}(\tau_1, \tau_2)]^{q-1}. \end{aligned} \quad (6)$$

Here the self-energy due to the rest of the chain is $\mathbf{D}_{K,L}$ [89], defined recursively by $\mathbf{D}_{0,L} = \sigma R_L \left(\frac{-i\Omega}{2t}\right) \sigma^\dagger$, and $\mathbf{D}_{K,L} = \left(-\frac{i\omega}{t} - \mathbf{D}_{K-1,L}\right)^{-1}$, using the Matsubara frequency matrices $\omega = \text{diag}(\omega_1^{(1)}, \omega_2^{(1)}, \dots, \omega_2^{(2)}, \omega_1^{(2)}, \dots)$, and $\Omega = \text{diag}(\Omega_1, \Omega_2, \dots)$. The twist operator σ transforms fields across the partition. In the frequency space, $\sigma(i\omega_m^{(a)}, i\Omega_n) = \int_{(a-1)\beta}^{a\beta} \frac{d\tau}{\sqrt{2\beta}} e^{i[\omega_m^{(a)} - \Omega_n]\tau}$, for replicas $a = 1, 2$.

Following (5), $S_2 = 2 \log Z - \log Z_{(2)}$ gives the second Rényi entropy. The ground-state entanglement simplifies after subtracting the zero S_2 when A and B are decoupled. Denote the partition function in a decoupled system by \check{Z} , we get

$$\begin{aligned} \frac{S_2}{N} &= \frac{1}{N} [2 \log Z - \log Z_{(2)} - (2 \log \check{Z} - \log \check{Z}_{(2)})] \quad (7) \\ &= -\frac{1}{2} \text{Tr} \log [G_{(2)}^{-1} \tilde{G}] + J^2 \left(\frac{1}{4q} - \frac{1}{4} \right) \\ &\quad \times \int d\tau_1 d\tau_2 \{ [2\tilde{G}(\tau_1, \tau_2)]^q - [2G_{(2)}(\tau_1, \tau_2)]^q \} \\ &\quad + \sum_{s=1,2} \frac{1}{2} \text{Tr} \log \left[\frac{1 - R_{L_s} \left(\frac{-i\omega}{2t}\right) R_{K_s} \left(\frac{-i\omega}{2t}\right)}{1 - \sigma R_{L_s} \left(\frac{-i\Omega}{2t}\right) \sigma^\dagger R_{K_s} \left(\frac{-i\omega}{2t}\right)} \right], \end{aligned}$$

where $\tilde{G} = G \otimes \mathbf{1}_2$ is the Green's function for Z , i.e. (1) with $K \rightarrow L_1 + K_1$ and $L \rightarrow L_2 + K_2$, replicated diagonally in the replica space. The last line is the entanglement between free Majorana chains with uniform nearest-neighbor hoppings.

Energy defect—Two distinct bipartitions for the Rényi entropy that reveal universal conformal data have been considered in the literature: i) where the defect is located deep inside one subsystem, say A ; ii) where the bipartition between two subsystems A and B is located at or near the defect. The first bipartition reveals the g function via a folding trick, i.e., the offset of Rényi entropy between the system with and without defect equals the boundary entropy of a folded system with doubled degrees of freedom [16, 94, 95]. In the second bipartition, the entanglement across the interface $S_2 \sim \frac{\tilde{c}_2}{8} \log L_A$, where L_A is the size of region A (for simplicity we set $L_B = L_A$). The prefactor \tilde{c}_2 defines the effective central charge, which can differ from the central charge of the bulk CFT. In a free fermion CFT, the effective central charge is a universal function of the transmission coefficient \mathcal{T} [52], i.e.,

$$\tilde{c}_2 = \frac{8}{\pi^2} \arcsin^2 \sqrt{\frac{\mathcal{T}}{2}}. \quad (8)$$

We shall see that this relation breaks down for an SYK defect.

Before returning to the SYK defect, we apply our method to evaluate the g function and the effective central charge for

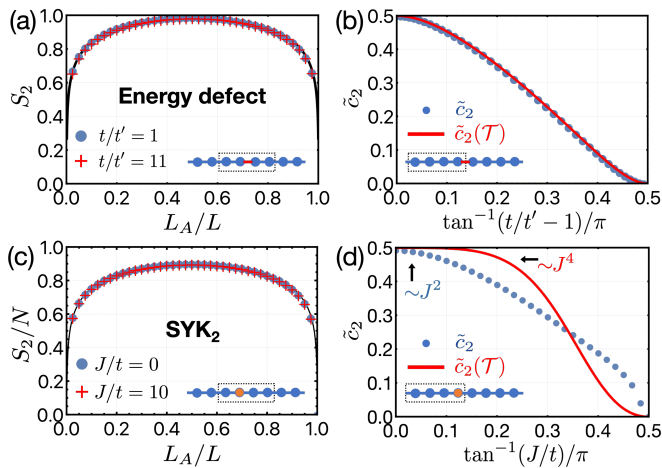


FIG. 4. The second Rényi entropy and the extracted effective central charge under different partition schemes, in the presence of (a)–(b) an energy defect with bond strength t' , and (c)–(d) SYK₂ coupling of strength J across N Majorana chains, both at the center of the chain. In (a) and (c), subsystem A is the center region. Black curves give the analytical result of Eq. (9) with $c_2 = 1/2$ and $L = 4000$. In (b) and (d), the partition is at the defect. The effective central charge is computed both from the logarithmic scaling of S_2 (dots) and from the transmission probability \mathcal{T} (line). Their disagreement in (d) signifies non-Gaussianity.

the energy defect as a warmup [15, 16, 56]. The energy defect in the Ising CFT can be modeled by replacing the SYK site by a bond defect with a distinct hopping amplitude t' [52, 56]. Let us set $N = 1$ since different chains do not couple in this case. With a slight modification, our saddle-point method can be applied to evaluate its Rényi entropy. The result is shown in Fig. 4(a)(b): Fig. 4(a) shows that $\log g = 0$ for the energy defect, and Fig. 4(b) shows the effective central charge, plotted along with the exact analytical result (8), with $\sqrt{\mathcal{T}} = \frac{2}{t'/t + t/t'}$. This benchmarks our method.

g function—To get the g function in the presence of the SYK₂ defect, we put it in the middle of region A in a symmetric setup, i.e., $L_1 = L_2$ and $K_1 = K_2$ in Fig. 3(a), and compute S_2 as the subsystem size fraction varies while the total length is fixed. Since the g function is universal, S_2 should depend logarithmically on L_A , the size of region A , with a constant offset when $\beta \gg L$ [44, 56],

$$\frac{S_2}{N} = \frac{c_2}{4} \log \left[\frac{L}{\pi} \sin \left(\frac{\pi L_A}{L} \right) \right] + s, \quad (9)$$

such that the constant $s = \log g$ is independent of the defect strength J . Here, the factor $c_2/4$ is the sum of the equal contribution $c_2/8$ from each of the two interfaces, and N comes from the large- N structure of the SYK. The universality of s is confirmed in Fig. 4(c), which shows no offset between the entropy curves at different J 's [96], up to even-odd effects [97–99]. This implies that $g = 1$, same as that of an energy defect [17].

Effective central charge—For the effective central charge due to the SYK defect, we partition our system at the SYK

site as depicted in Fig. 3(c). The result is a dCFT determined by the bulk free CFTs and the SYK defect [50]. The second Rényi entanglement entropy across the SYK defect is $\frac{S_2}{N} \sim \frac{\tilde{c}_2}{8} \log L_A$ [49, 52–54]. Thus, we enlarge the system symmetrically in A and B to extract \tilde{c}_2 . As seen in Fig. 4(d), \tilde{c}_2 decreases towards zero at stronger J until the two sides decouple. Therefore, the marginal SYK₂ interaction induces an interface CFT with a continuously tunable effective central charge. For irrelevant cases of $q > 2$, the \tilde{c}_2 remains at $1/2$, that of a free Majorana chain or Ising CFT. A relevant coupling reduces \tilde{c}_2 to zero at low temperature, as is the case of massless bosonic chains with an SYK [89] or mass defect [100], although the former is unstable [84, 101–103]. Finite- N calculations confirm the $q = 2$ result qualitatively.

In contrast to free dCFTs, the transmission coefficient and the effective central charge are not related by (8) for the SYK₂ defect, which is clear from Fig. 4(d). The disagreement signifies the deviation from Gaussian defects due to the disorder averaging of SYK₂, even though each random realization is noninteracting.

Concluding remarks—We have presented a novel family of boundary and defect CFTs, built from the SYK interaction coupling 1+1D systems, that exhibits a tunable effective central charge. Based on path integral and functional determinant, we devised a versatile method to compute the (conformal) data of defects embedded in 1+1D. Our method admits arbitrary partitions of the system, and scales economically to low temperature and large systems. It can be extended to models with different boundary conditions, next-nearest-neighbor hoppings, etc. With this method, we evaluated the boundary entropy and effective central charge of the dCFT built from the SYK interaction. Our findings suggest that it extends beyond all known Gaussian dCFTs.

While our primary focus is on the defect of the Ising CFT or free Majorana chain, it is worth emphasizing that our construction can be readily generalized to other large- N models, including interacting ones. One example is the bosonic SYK defect, where a relevant defect coupling renders total reflection. Another is the Yukawa-SYK defect [104, 105]. More importantly, nontrivial self-energy can be further incorporated to study cases with interacting bulk CFTs [89]. Beyond SYK-like models, our construction also opens an interesting arena to realize new defect states in CFTs such as the minimal models [26]. For instance, random couplings between primary fields from N identical copies of a minimal model could lead to a nontrivial renormalization group flow. We leave a detailed study for future work.

Acknowledgements—We thank Xiao-Yang Shen for helpful discussions on the bosonic SYK model. This work is supported by a startup grant from Tulane University.

* sjian@tulane.edu

[1] J. L. Cardy, Conformal invariance and surface critical behav-

- ior, *Nucl. Phys. B* **240**, 514 (1984).
- [2] J. L. Cardy, Boundary conditions, fusion rules and the verlinde formula, *Nucl. Phys. B* **324**, 581 (1989).
- [3] N. Andrei, A. Bissi, M. Buican, J. Cardy, P. Dorey, N. Drukker, J. Erdmenger, D. Friedan, D. Fursaev, A. Konechny, C. Kristjansen, I. Makabe, Y. Nakayama, A. O'Bannon, R. Parini, B. Robinson, S. Ryu, C. Schmidt-Colinet, V. Schomerus, C. Schweigert, and G. M. T. Watts, Boundary and defect CFT: open problems and applications, *J. Phys. A* **53**, 453002 (2020).
- [4] M. Z. Hasan and C. L. Kane, Colloquium: Topological insulators, *Rev. Mod. Phys.* **82**, 3045 (2010).
- [5] X.-L. Qi and S.-C. Zhang, Topological insulators and superconductors, *Rev. Mod. Phys.* **83**, 1057 (2011).
- [6] A. Recknagel and V. Schomerus, *Boundary Conformal Field Theory and the Worldsheet Approach to D-Branes* (Cambridge University Press, 2013).
- [7] J. Polchinski, TASI lectures on D-branes, [arXiv:hep-th/9611050](https://arxiv.org/abs/hep-th/9611050) (1996).
- [8] J. Maldacena, The large- N limit of superconformal field theories and supergravity, *Int. J. Theor. Phys.* **38**, 1113 (1999).
- [9] E. Witten, Anti de Sitter space and holography, *Adv. Theor. Math. Phys.* **2**, 253 (1998).
- [10] S. S. Gubser, I. R. Klebanov, and A. M. Polyakov, Gauge theory correlators from non-critical string theory, *Phys. Lett.* **428**, 105 (1998).
- [11] T. Takayanagi, Holographic dual of a boundary conformal field theory, *Phys. Rev. Lett.* **107**, 101602 (2011).
- [12] M. Fujita, T. Takayanagi, and E. Tonni, Aspects of Ads/BCFT, *J. High Energy Phys.* **2011** (11), 43.
- [13] C. L. Kane and M. P. A. Fisher, Transmission through barriers and resonant tunneling in an interacting one-dimensional electron gas, *Phys. Rev. B* **46**, 15233 (1992).
- [14] T. Quella, I. Runkel, and G. M. T. Watts, Reflection and transmission for conformal defects, *J. High Energy Phys.* **2007** (04), 095.
- [15] M. Oshikawa and I. Affleck, Defect lines in the Ising model and boundary states on orbifolds, *Phys. Rev. Lett.* **77**, 2604 (1996).
- [16] M. Oshikawa and I. Affleck, Boundary conformal field theory approach to the critical two-dimensional Ising model with a defect line, *Nucl. Phys. B* **495**, 533 (1997).
- [17] G. Delfino, G. Mussardo, and P. Simonetti, Scattering theory and correlation functions in statistical models with a line of defect, *Nucl. Phys. B* **432**, 518 (1994).
- [18] C. Bachas, J. de Boer, R. Dijkgraaf, and H. Ooguri, Permeable conformal walls and holography, *J. High Energy Phys.* **2002** (06), 027.
- [19] C. Bachas, I. Brunner, and D. Roggenkamp, Fusion of critical defect lines in the 2d Ising model, *J. Stat. Mech.* **2013**, P08008 (2013).
- [20] J. Fröhlich, J. Fuchs, I. Runkel, and C. Schweigert, Kramers-Wannier duality from conformal defects, *Phys. Rev. Lett.* **93**, 070601 (2004).
- [21] J. Fröhlich, J. Fuchs, I. Runkel, and C. Schweigert, Duality and defects in rational conformal field theory, *Nucl. Phys. B* **763**, 354 (2007).
- [22] T. Quella and V. Schomerus, Symmetry breaking boundary states and defect lines, *J. High Energy Physics* **2002**, 028 (2002).
- [23] S. Fredenhagen and T. Quella, Generalised permutation branes, *J. High Energy Phys.* **2005** (11), 004.
- [24] I. Brunner and M. R. Gaberdiel, Matrix factorisations and permutation branes, *J. High Energy Physics* **2005**, 012 (2005).
- [25] I. Makabe and G. M. T. Watts, Defects in the Tricritical Ising model, *J. High Energy Phys.* **2017** (09), 013, [arXiv:1703.09148 \[hep-th\]](https://arxiv.org/abs/1703.09148).
- [26] M. Jeng and A. W. W. Ludwig, Random defect lines in conformal minimal models, *Nucl. Phys. B* **594**, 685 (2001).
- [27] L. Hu, Y.-C. He, and W. Zhu, Solving conformal defects in 3D conformal field theory using fuzzy sphere regularization, *Nat. Commun.* **15**, 3659 (2024).
- [28] M. A. Metlitski, Boundary criticality of the $O(N)$ model in $d = 3$ critically revisited, *SciPost Phys.* **12**, 131 (2022).
- [29] F. Parisen Toldin and M. A. Metlitski, Boundary criticality of the 3d $O(N)$ model: From normal to extraordinary, *Phys. Rev. Lett.* **128**, 215701 (2022).
- [30] A. Krishnan and M. A. Metlitski, A plane defect in the 3d $O(N)$ model, *SciPost Phys.* **15**, 090 (2023).
- [31] S. Giombi and B. Liu, Notes on a surface defect in the $O(N)$ model, *J. High Energy Phys.* **2023** (12), 4.
- [32] M. Trépanier, Surface defects in the $O(N)$ model, *J. High Energy Phys.* **2023** (9), 74.
- [33] A. Raviv-Moshe and S. Zhong, Phases of surface defects in scalar field theories, *J. High Energy Phys.* **2023** (8), 143.
- [34] N. R. Constable, R. C. Myers, and Ø. Tafjord, Noncommutative bion core, *Phys. Rev. D* **61**, 106009 (2000).
- [35] A. Karch and L. Randall, Locally localized gravity, *J. High Energy Phys.* **2001** (05), 008.
- [36] O. DeWolfe, D. Z. Freedman, and H. Ooguri, Holography and defect conformal field theories, *Phys. Rev. D* **66**, 025009 (2002).
- [37] J. Erdmenger, Z. Guralnik, and I. Kirsch, Four-dimensional superconformal theories with interacting boundaries or defects, *Phys. Rev. D* **66**, 025020 (2002).
- [38] I. Affleck and A. W. W. Ludwig, The Kondo effect, conformal field theory and fusion rules, *Nucl. Phys. B* **352**, 849 (1991).
- [39] L. Amico, R. Fazio, A. Osterloh, and V. Vedral, Entanglement in many-body systems, *Rev. Mod. Phys.* **80**, 517 (2008).
- [40] R. Horodecki, P. Horodecki, M. Horodecki, and K. Horodecki, Quantum entanglement, *Rev. Mod. Phys.* **81**, 865 (2009).
- [41] P. Calabrese, J. Cardy, and B. Doyon, Entanglement entropy in extended quantum systems, *J. Phys. A* **42**, 500301 (2009).
- [42] J. Eisert, M. Cramer, and M. B. Plenio, Colloquium: Area laws for the entanglement entropy, *Rev. Mod. Phys.* **82**, 277 (2010).
- [43] P. Jizba and T. Arimitsu, The world according to Rényi: Thermodynamics of multifractal systems, *Ann. Phys. (N. Y.)* **312**, 17 (2004).
- [44] P. Calabrese and J. Cardy, Entanglement entropy and quantum field theory, *J. Stat. Mech.* **2004**, P06002 (2004).
- [45] P. Calabrese and J. Cardy, Entanglement entropy and conformal field theory, *J. Phys. A* **42**, 504005 (2009).
- [46] H. W. J. Blöte, J. L. Cardy, and M. P. Nightingale, Conformal invariance, the central charge, and universal finite-size amplitudes at criticality, *Phys. Rev. Lett.* **56**, 742 (1986).
- [47] I. Affleck, Universal term in the free energy at a critical point and the conformal anomaly, *Phys. Rev. Lett.* **56**, 746 (1986).
- [48] I. Affleck and A. W. W. Ludwig, Universal noninteger "ground-state degeneracy" in critical quantum systems, *Phys. Rev. Lett.* **67**, 161 (1991).
- [49] K. Sakai and Y. Satoh, Entanglement through conformal interfaces, *J. High Energy Phys.* **2008** (12), 001.
- [50] V. Eisler and I. Peschel, Entanglement in fermionic chains with interface defects, *Ann. Phys. (Berlin)* **522**, 679 (2010).
- [51] P. Calabrese, M. Mintchev, and E. Vicari, Entanglement entropy of quantum wire junctions, *J. Phys. A* **45**, 105206 (2012).
- [52] I. Peschel and V. Eisler, Exact results for the entanglement

- across defects in critical chains, *J. Phys. A* **45**, 155301 (2012).
- [53] E. Brehm and I. Brunner, Entanglement entropy through conformal interfaces in the 2d Ising model, *J. High Energy Phys.* **2015** (9), 080.
- [54] L. Capizzi, S. Murciano, and P. Calabrese, Rényi entropy and negativity for massless Dirac fermions at conformal interfaces and junctions, *J. High Energy Phys.* **2022** (8), 171.
- [55] L. Capizzi, S. Murciano, and P. Calabrese, Rényi entropy and negativity for massless complex boson at conformal interfaces and junctions, *J. High Energy Phys.* **2022** (11), 105.
- [56] D. Rogerson, F. Pollmann, and A. Roy, Entanglement entropy and negativity in the Ising model with defects, *J. High Energy Phys.* **2022** (6).
- [57] A. Roy and H. Saleur, Entanglement entropy in the Ising model with topological defects, *Phys. Rev. Lett.* **128**, 090603 (2022).
- [58] S. Sachdev and J. Ye, Gapless spin-fluid ground state in a random quantum Heisenberg magnet, *Phys. Rev. Lett.* **70**, 3339 (1993).
- [59] A. Kitaev, [A simple model of quantum holography](#), Kavli Institute for Theoretical Physics Program: Entanglement in Strongly-Correlated Quantum Matter, id. 2 and 38 (2015).
- [60] J. Maldacena and D. Stanford, Remarks on the Sachdev-Ye-Kitaev model, *Phys. Rev. D* **94**, 106002 (2016).
- [61] J. Polchinski and V. Rosenhaus, The spectrum in the Sachdev-Ye-Kitaev model, *J. High Energy Phys.* **2016** (4), 1.
- [62] D. Chowdhury, A. Georges, O. Parcollet, and S. Sachdev, Sachdev-Ye-Kitaev models and beyond: Window into non-Fermi liquids, *Rev. Mod. Phys.* **94**, 035004 (2022).
- [63] X.-Y. Song, C.-M. Jian, and L. Balents, Strongly correlated metal built from Sachdev-Ye-Kitaev models, *Phys. Rev. Lett.* **119**, 216601 (2017).
- [64] Z. Bi, C.-M. Jian, Y.-Z. You, K. A. Pawlak, and C. Xu, Instability of the non-Fermi-liquid state of the Sachdev-Ye-Kitaev model, *Phys. Rev. B* **95**, 205105 (2017).
- [65] S.-K. Jian, Z.-Y. Xian, and H. Yao, Quantum criticality and duality in the Sachdev-Ye-Kitaev/AdS₂ chain, *Phys. Rev. B* **97**, 205141 (2018).
- [66] D. Chowdhury, Y. Werman, E. Berg, and T. Senthil, Translationally invariant non-Fermi-liquid metals with critical Fermi surfaces: Solvable models, *Phys. Rev. X* **8**, 031024 (2018).
- [67] A. A. Patel, J. McGreevy, D. P. Arovas, and S. Sachdev, Magnetotransport in a model of a disordered strange metal, *Phys. Rev. X* **8**, 021049 (2018).
- [68] Y.-Z. You, A. W. W. Ludwig, and C. Xu, Sachdev-Ye-Kitaev model and thermalization on the boundary of many-body localized fermionic symmetry-protected topological states, *Phys. Rev. B* **95**, 115150 (2017).
- [69] S.-K. Jian and H. Yao, Solvable Sachdev-Ye-Kitaev models in higher dimensions: From diffusion to many-body localization, *Phys. Rev. Lett.* **119**, 206602 (2017).
- [70] J. Sonner and M. Vielma, Eigenstate thermalization in the Sachdev-Ye-Kitaev model, *J. High Energy Phys.* **2017** (11), 149.
- [71] Y. Gu, A. Lucas, and X.-L. Qi, Spread of entanglement in a Sachdev-Ye-Kitaev chain, *J. High Energy Phys.* **2017** (9), 120.
- [72] A. M. García-García, B. Loureiro, A. Romero-Bermúdez, and M. Tezuka, Chaotic-integrable transition in the Sachdev-Ye-Kitaev model, *Phys. Rev. Lett.* **120**, 241603 (2018).
- [73] C. Liu, X. Chen, and L. Balents, Quantum entanglement of the Sachdev-Ye-Kitaev models, *Phys. Rev. B* **97**, 245126 (2018).
- [74] X. Dai, S.-K. Jian, and H. Yao, Global phase diagram of the one-dimensional Sachdev-Ye-Kitaev model at finite N , *Phys. Rev. B* **100**, 235144 (2019).
- [75] C. Liu, P. Zhang, and X. Chen, Non-unitary dynamics of Sachdev-Ye-Kitaev chain, *SciPost Phys.* **10**, 048 (2021).
- [76] P. Zhang, S.-K. Jian, C. Liu, and X. Chen, Emergent replica conformal symmetry in non-Hermitian SYK₂ chains, *Quantum* **5**, 579 (2021).
- [77] S.-K. Jian, C. Liu, X. Chen, B. Swingle, and P. Zhang, Measurement-induced phase transition in the monitored Sachdev-Ye-Kitaev model, *Phys. Rev. Lett.* **127**, 140601 (2021).
- [78] A. M. García-García, Y. Jia, D. Rosa, and J. J. M. Verbaarschot, Replica symmetry breaking in random non-Hermitian systems, *Phys. Rev. D* **105**, 126027 (2022).
- [79] A. M. García-García, Y. Jia, D. Rosa, and J. J. M. Verbaarschot, Dominance of replica off-diagonal configurations and phase transitions in a PT symmetric Sachdev-Ye-Kitaev model, *Phys. Rev. Lett.* **128**, 081601 (2022).
- [80] G. Penington, S. H. Shenker, D. Stanford, and Z. Yang, Replica wormholes and the black hole interior, *J. High Energy Phys.* **2022** (3), 205.
- [81] A. Almheiri, T. Hartman, J. Maldacena, E. Shaghoulian, and A. Tajdini, Replica wormholes and the entropy of Hawking radiation, *J. High Energy Phys.* **2020** (5), 13.
- [82] Y. Chen, X.-L. Qi, and P. Zhang, Replica wormhole and information retrieval in the SYK model coupled to Majorana chains, *J. High Energy Phys.* **2020** (6), 121.
- [83] Y. Liu, Z.-Y. Xian, C. Peng, and Y. Ling, Black holes entangled by radiation, *J. High Energy Phys.* **2022** (9), 179.
- [84] X.-Y. Shen, Long range SYK model and boundary SYK model, [arXiv:2308.12598](#) (2023).
- [85] Q. Gao, P. Zhang, and X. Chen, Information scrambling in free fermion systems with a sole interaction, *Phys. Rev. B* **110**, 035137 (2024).
- [86] Q. Gao, T. Zhou, P. Zhang, and X. Chen, Scrambling transition in free fermion systems induced by a single impurity, *Phys. Rev. B* **110**, 235110 (2024).
- [87] D. Bagrets, A. Altland, and A. Kamenev, Sachdev-Ye-Kitaev model as Liouville quantum mechanics, *Nucl. Phys. B* **911**, 191 (2016).
- [88] A. Kitaev and S. J. Suh, The soft mode in the Sachdev-Ye-Kitaev model and its gravity dual, *J. High Energy Phys.* **2018** (5), 183.
- [89] See Supplemental Material for further details.
- [90] R. K. Mallik, The inverse of a tridiagonal matrix, *Linear Algebra Appl.* **325**, 109 (2001).
- [91] X. Zhang, *Matrix Analysis and Applications*, 2nd ed. (Tsinghua University Press, Beijing, China, 2013).
- [92] Y. Komijani and P. Coleman, Model for a ferromagnetic quantum critical point in a 1D Kondo lattice, *Phys. Rev. Lett.* **120**, 157206 (2018).
- [93] S. Shao and Y. Komijani, Towards entanglement entropy of random large- N theories, *Phys. Rev. D* **109**, 016015 (2024).
- [94] H. Saleur, Lectures on non perturbative field theory and quantum impurity problems, in *Aspects Topologiques de la Physique en Basse Dimension. Topological Aspects of Low Dimensional Systems*, edited by A. Comtet, T. Jolicœur, S. Ouvry, and F. David (Springer, Berlin, Heidelberg, 1999).
- [95] M. Gutperle and J. D. Miller, A note on entanglement entropy for topological interfaces in RCFTs, *J. High Energy Phys.* **2016** (4), 176.
- [96] A J -independent offset is added to the analytical curve in Fig. 4(c) to match the result at $J = 0$. This offset comes from the imperfect mirror symmetry in even-length Majorana chains coupled at the SYK site, as seen in the insets of Fig. 4. In contrast, no offset to the logarithm is needed for the energy

defect in Fig. 4(a).

- [97] M. Fagotti and P. Calabrese, Universal parity effects in the entanglement entropy of XX chains with open boundary conditions, *J. Stat. Mech.* **2011**, P01017 (2011).
- [98] N. Laflorencie, E. S. Sørensen, M.-S. Chang, and I. Affleck, Boundary effects in the critical scaling of entanglement entropy in 1D systems, *Phys. Rev. Lett.* **96**, 100603 (2006).
- [99] I. Affleck, N. Laflorencie, and E. S. Sørensen, Entanglement entropy in quantum impurity systems and systems with boundaries, *J. Phys. A* **42**, 504009 (2009).
- [100] H. J. Lipkin, Scattering theory for pedestrians, in *Quantum Mechanics: New Approaches to Selected Topics* (American Elsevier, New York, 1973) Chap. 8.
- [101] J. Murugan, D. Stanford, and E. Witten, More on supersymmetric and 2d analogs of the SYK model, *J. High Energy Phys.* **2017** (8), 146.
- [102] J. Liu, E. Perlmutter, V. Rosenhaus, and D. Simmons-Duffin, d -dimensional SYK, AdS loops, and $6j$ symbols, *J. High Energy Phys.* **2019** (3), 52.
- [103] E. Tulipman and E. Berg, Strongly coupled quantum phonon fluid in a solvable model, *Phys. Rev. Res.* **2**, 033431 (2020).
- [104] Y. Wang, Solvable strong-coupling quantum-dot model with a non-Fermi-liquid pairing transition, *Phys. Rev. Lett.* **124**, 017002 (2020).
- [105] Y. Ge and S.-K. Jian, (to be published).

SUPPLEMENTAL MATERIAL

I. DERIVATION OF THE LARGE- N ACTION

The model is given by the Hamiltonian $H = H_{\text{CFT}} + H_{\text{I}}$, where H_{CFT} consists of N decoupled Majorana chains,

$$H_{\text{CFT}} = -i2t \sum_r \psi_{j,r} \psi_{j,r+1}, \quad (\text{S1})$$

and H_{I} denotes the interface given by SYK interaction

$$H_{\text{I}} = i^{q/2} \sum_{j_1, \dots, j_q} J_{j_1, \dots, j_q} \psi_{j_1, 0} \dots \psi_{j_q, 0}. \quad (\text{S2})$$

Here, r is the site index, and $j = 1, \dots, N$ denotes the flavor of Majorana at each site. Namely, each site has N Majorana fermions. $\psi_{j,r}$ denotes the j -th Majorana fermion at site r , and $\{\psi_{j,r}, \psi_{j',r'}\} = \delta_{j,j'} \delta_{r,r'}$. t is the hopping amplitude between nearest-neighbor sites. The SYK interaction that couples different chains exists at the site $r = 0$. We refer to it as the SYK site.

The interaction strength J_{j_1, \dots, j_q} is a Gaussian variable with mean zero and variance

$$\overline{J_{j_1, \dots, j_q} J_{j'_1, \dots, j'_q}} = \delta_{j_1, j'_1} \dots \delta_{j_q, j'_q} \frac{2^{q-1} J^2 (q-1)!}{N^{q-1}}. \quad (\text{S3})$$

Define the hopping matrix $h_{r_1, r_2} = \delta_{r_2, r_1+1} - \delta_{r_2, r_1-1}$. The action is thus

$$-I = -\frac{1}{2} \sum_{j, r_1, r_2} \int d\tau \psi_{j, r_1}(\tau) (\partial_\tau \delta_{r_1, r_2} - i t h_{r_1, r_2}) \psi_{j, r_2}(\tau) + \int d\tau i^{q/2} \sum_{j_1, \dots, j_q} J_{j_1, \dots, j_q} \psi_{j_1, 0} \dots \psi_{j_q, 0}. \quad (\text{S4})$$

After integrating over the Gaussian distributed interaction, the action reads

$$-I = -\frac{1}{2} \sum_{j, r_1, r_2} \int d\tau \psi_{j, r_1}(\tau) (\partial_\tau \delta_{r_1, r_2} - i t h_{r_1, r_2}) \psi_{j, r_2}(\tau) + \frac{N J^2}{4q} \int d\tau_1 d\tau_2 \left(2 \frac{1}{N} \sum_j \psi_{j, 0}(\tau_1) \psi_{j, 0}(\tau_2) \right)^q, \quad (\text{S5})$$

To derive the (G, Σ) action, we introduce the bilocal fields $G(\tau_1, \tau_1)$, $\Sigma(\tau_1, \tau_2)$ and multiply the partition function by a constant [60, 71, 87, 88],

$$1 = \int \mathcal{D}G \mathcal{D}\Sigma e^{-\frac{N}{2} \int d\tau_1 d\tau_2 G(\tau_1, \tau_2) \Sigma(\tau_1, \tau_2)} = \int \mathcal{D}G \delta[G(\tau_1, \tau_2)]. \quad (\text{S6})$$

Here the measure $\mathcal{D}G \mathcal{D}\Sigma \sim \prod_{\tau_1, \tau_2} \frac{N}{2\pi} dG(\tau_1, \tau_2) d[i\Sigma(\tau_1, \tau_2)]$. Then we shift $G(\tau_1, \tau_2) \rightarrow G(\tau_1, \tau_2) - \sum_j \psi_{j, 0}(\tau_1) \psi_{j, 0}(\tau_2) / N$. By virtual of the delta function, G plays the role of the Majorana propagator. This also shifts the quadratic Hamiltonian by Σ , which one can later identify with the self-energy in the Schwinger-Dyson equation (S9). The result is

$$\begin{aligned} -I &= -\frac{1}{2} \sum_{j, r_1, r_2} \int d\tau_1 d\tau_2 \psi_{j, r_1}(\tau_1) [(\partial_{\tau_1} \delta_{r_1, r_2} - i t h_{r_1, r_2}) \delta(\tau_1 - \tau_2) - \delta_{r_1, 0} \delta_{r_2, 0} \Sigma(\tau_1, \tau_2)] \psi_{j, r_2}(\tau_2) \\ &\quad - \frac{N}{2} \int d\tau_1 d\tau_2 G(\tau_1, \tau_2) \Sigma(\tau_1, \tau_2) + \frac{N J^2}{4q} \int d\tau_1 d\tau_2 [2G(\tau_1, \tau_2)]^q. \end{aligned} \quad (\text{S7})$$

It is not hard to check that, by integrating over G and Σ , this reduces to the fermionic action. Now the action is only quadratic in terms of Majorana fermions, so we can integrate them out to get

$$-\frac{I}{N} = \frac{1}{2} \log \det [(\partial_{\tau_1} \delta_{r_1, r_2} - ith_{r_1, r_2}) \delta(\tau_1 - \tau_2) - \delta_{r_1, 0} \delta_{r_2, 0} \Sigma(\tau_1, \tau_2)] - \frac{1}{2} \int d\tau_1 d\tau_2 G(\tau_1, \tau_2) \Sigma(\tau_1, \tau_2) + \frac{J^2}{4q} \int d\tau_1 d\tau_2 [2G(\tau_1, \tau_2)]^q. \quad (\text{S8})$$

The determinant involves matrices whose indices range over the imaginary time and the lattice sites. Since the action has a large- N structure, we can implement a saddle point analysis. The Schwinger-Dyson equations read

$$G(\tau_1, \tau_2) = (\partial_{\tau} - \Sigma - ith)_{00}^{-1}(\tau_1, \tau_2), \quad \Sigma(\tau_1, \tau_2) = J^2 [2G(\tau_1, \tau_2)]^{q-1}, \quad (\text{S9})$$

where the first equation should be understood as a matrix equation. The subscript denotes $r_1 = 0, r_2 = 0$ component.

We can further simplify the action by noting that the self-energy is nontrivial only at the SYK site. We assume the solution to be time translationally symmetric, i.e., $G(\tau_1, \tau_2) = G(\tau_1 - \tau_2)$, $\Sigma(\tau_1, \tau_2) = \Sigma(\tau_1 - \tau_2)$. In this case, we can perform a Fourier transformation in the imaginary time domain, i.e.,

$$G(\tau_1, \tau_2) = \frac{1}{\beta} \sum_n e^{i\omega_n(\tau_1 - \tau_2)} G(i\omega_n), \quad \Sigma(\tau_1, \tau_2) = \frac{1}{\beta} \sum_n e^{i\omega_n(\tau_1 - \tau_2)} \Sigma(i\omega_n), \quad \omega_n = \frac{(2n+1)\pi}{\beta}. \quad (\text{S10})$$

We consider the open boundary condition for these Majorana chains. In the frequency space, the matrix inside the determinant becomes tridiagonal in the basis of $\psi_r(i\omega_n)$ at each Matsubara frequency,

$$\mathcal{M}_{rr'} = \bigoplus_n [-i\omega_n \delta_{rr'} - \Sigma(i\omega_n) \delta_{r,0} \delta_{0,r'} - it\delta_{r+1,r'} + it\delta_{r,r'+1}]. \quad (\text{S11})$$

The determinant of a tridiagonal matrix has a simple analytical expression [90]. Therefore, we can first evaluate the determinant at each frequency, and then take the product over all the frequencies. After a straightforward calculation, the large- N action can be simplified as

$$-\frac{I}{N} = \frac{1}{2} \log \prod_n \left[-i\omega_n - \Sigma(i\omega_n) - tR_K \left(\frac{-i\omega_n}{2t} \right) - tR_L \left(\frac{-i\omega_n}{2t} \right) \right] - \frac{1}{2} \int d\tau_1 d\tau_2 G(\tau_1, \tau_2) \Sigma(\tau_1, \tau_2) + \frac{J^2}{4q} \int d\tau_1 d\tau_2 [2G(\tau_1, \tau_2)]^q + \frac{I'}{N}. \quad (\text{S12})$$

where $R_L(x) = \frac{U_{L-1}(x)}{U_L(x)}$, and U_L is the Chebyshev polynomial of the second kind. $K-1$ and L are the number of sites to the left and right of the SYK sites, respectively, as shown in Fig. 1. The term

$$\frac{I'}{N} = \frac{1}{2} \sum_n \log \left[t^{L+K} U_L \left(\frac{-i\omega_n}{2t} \right) U_K \left(\frac{-i\omega_n}{2t} \right) \right] \quad (\text{S13})$$

is independent of G and Σ . Varying the bilocal fields, we obtain the corresponding Schwinger-Dyson equation

$$G(i\omega_n) = \left[-i\omega_n - \Sigma(i\omega_n) - tR_K \left(\frac{-i\omega_n}{2t} \right) - tR_L \left(\frac{-i\omega_n}{2t} \right) \right]^{-1}, \quad (\text{S14})$$

$$\Sigma(\tau_1, \tau_2) = J^2 [2G(\tau_1, \tau_2)]^{q-1}. \quad (\text{S15})$$

The effect of coupling to the Majorana chain is reflected in the correction to the self-energy in the form of ratios of the Chebyshev polynomials. Finally, we note that in the numerics, the ratio of U_L 's with large L 's can be numerically unstable, and the recursive relation $R_L(x) = 1/[2x - R_{L-1}(x)]$ may be helpful.

II. COMPUTE THE GREEN'S FUNCTION AT $L = \infty$ FOR ANY q

Here we derive in detail the large- N Green's function and self-energy of infinitely long SYK $_q$ -coupled Majorana chains, which are Eqs. (S14) and (S15) or Eqs. (1) in the main text. To proceed, we consider an infinite number of sites to the left and right of the SYK point, i.e., $L, K \rightarrow \infty$. Observing that

$$\lim_{L \rightarrow \infty} R_L(x) = x - \sqrt{x^2 - 1}, \quad (\text{S16})$$

the Schwinger-Dyson equation (S14) becomes

$$G(i\omega_n) = \left[\sqrt{-4t^2 - \omega_n^2} - \Sigma(i\omega_n) \right]^{-1}. \quad (\text{S17})$$

Note that $\sqrt{-4t^2 - \omega_n^2}$ is simply the $G^{-1}(i\omega_n)$ of a 1D chain. Unlike the SYK model, the coupling to the Majorana chain is relevant at small frequencies for $q > 2$, while the SYK $_q$ type of interaction is irrelevant for $q > 2$. Therefore, we consider SYK $_2$ where the interaction is marginal. To this end, we eliminate $\Sigma(i\omega_n)$ so that

$$G(i\omega_n) = \left[\sqrt{-4t^2 - \omega_n^2} - 2J^2 G(i\omega_n) \right]^{-1}. \quad (\text{S18})$$

Solving it for the advanced Green's function gives

$$G(\omega - i\eta) = \frac{i}{4J^2} \left[\sqrt{4t^2 - (\omega - i\eta)^2} - \sqrt{4t^2 + 8J^2 - (\omega - i\eta)^2} \right]. \quad (\text{S19})$$

The associated spectral function is shown in Fig. 2(a).

For the interacting cases $q > 2$, we expand G using its spectral function $A(\omega) = 2G''(\omega - i\eta)$ in Eq. (S19). The result for the self-energy at any q is

$$\Sigma_q''(\omega - i\eta) = J^2 \int \left[\prod_{i=1}^{q-2} \frac{d\nu_i}{\pi} A(\nu_i) \right] A \left(\omega - \sum_{j=1}^{q-2} \nu_j \right) \prod_{k=1}^{q-2} \left[n_{\zeta_k} \left(\sum_{l=k}^{q-2} \nu_l - \omega \right) - n_F(\nu_k) \right], \quad (\text{S20})$$

where

$$n_{\zeta_i}(\nu) = \begin{cases} -n_B(\nu), & i \in 2\mathbb{Z}, \\ n_F(\nu), & i \in 2\mathbb{Z} + 1. \end{cases} \quad (\text{S21})$$

Hilbert transform of the spectral function recovers the full Green's function. Numerical computations of the integrals can be formulated into convolutions that are expedited with the fast Fourier transform. For example, the self-energy of SYK $_4$ is given by multiplications and convolutions in real frequencies. Let the convolution be denoted by $*$, and omit the frequency arguments of A , n_F , and n_B , as they are identical. The expression for the self-energy is then given by

$$\Sigma_4''(\omega - i\eta) = \frac{J^2}{\pi^2} [(n_F A) * A * A + \{[(1 - 2n_F)A] * A\} \{1 + n_B\} * A]. \quad (\text{S22})$$

The local spectral function at the SYK $_4$ site is shown in Fig. 2(b)(c). Note that at high temperature, the Majorana chain-coupled SYK $_4$ dot behaves similarly to a 0+1D SYK dot. At low temperature, it flows away from the SYK point.

III. DERIVATION OF THE SECOND RÉNYI ENTROPY

To compute the Rényi entropy, we first assume that the chains satisfy an open boundary condition. Then, we divide the system into two regions, A and B. We are interested in the entanglement entropy between these two regions. The computation of entanglement entropy employs the replica trick [44]. Below, we first review the replica trick and then derive the Rényi entanglement entropy for the 1+1D chains.

A. Review of the replica trick

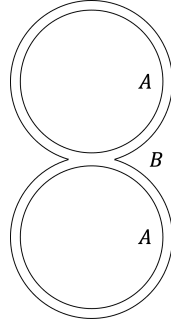
We consider the thermal density matrix $\rho = \frac{e^{-\beta H}}{Z}$, $Z = \text{Tr}(e^{-\beta H})$. The second Rényi entropy of the region A is

$$S_2 = -\log \text{Tr}_A[(\text{Tr}_B \rho)^2] = -\log \frac{Z_{(2)}}{Z^2}. \quad (\text{S23})$$

Here, $Z_{(2)}$ denotes a path integral with a twist boundary condition on the region A . In terms of replica fields, the boundary condition reads

$$\psi_{j \in A}^{(1)}(\beta) = -\psi_{j \in A}^{(1)}(0), \quad \psi_{j \in A}^{(2)}(\beta) = -\psi_{j \in A}^{(2)}(0), \quad (\text{S24})$$

$$\psi_{j \in B}^{(1)}(\beta) = \psi_{j \in B}^{(2)}(0), \quad \psi_{j \in B}^{(2)}(\beta) = -\psi_{j \in B}^{(1)}(0), \quad (\text{S25})$$



Supplementary Figure S1. The imaginary time contour for the second Rényi entropy. The fermionic field in a closed contour satisfies the conventional anti-periodic boundary condition, that leads to the fermionic Matsubara frequency.

where the superscripts 1, 2 denote the two replicas. The imaginary time contour for $Z_{(2)}$ is shown in Fig. S1. The fermionic field in a closed contour satisfies the conventional anti-periodic boundary condition that gives rise to the fermionic Matsubara frequency. A crucial point is that the closed imaginary-time contours of the fermionic fields in regions A and B have different periods. To this end, we introduce a different parametrization of the imaginary time contour, $s \in (0, 2\beta)$, such that $s < \beta$ ($s > \beta$) denotes the first (second) replica, i.e.,

$$\psi_j(s) = \begin{cases} \psi_j^{(1)}(s), & s \in (0, \beta), \\ \psi_j^{(2)}(s - \beta), & s \in (\beta, 2\beta). \end{cases} \quad (\text{S26})$$

The boundary condition now becomes

$$\psi_{j \in A}(\beta_-) = -\psi_{j \in A}(0_+), \quad \psi_{j \in A}(2\beta_-) = -\psi_{j \in A}(\beta_+), \quad \psi_{j \in B}(2\beta_-) = -\psi_{j \in A}(0_+). \quad (\text{S27})$$

The fermionic field in the region A can be expanded using the fermionic mode with the Matsubara frequency $\Omega_n = \frac{(2n+1)\pi}{2\beta}$, while the fermionic field in the region B needs to be expanded by two fermionic modes with the Matsubara frequency $\omega_n = \frac{(2n+1)\pi}{\beta}$. More explicitly, we have the following expansions,

$$\psi_{j \in A}(s) = \frac{1}{\sqrt{\beta}} \sum_n \left[\psi_{j \in A}^{(1)}(i\omega_n) e^{-i\omega_n s} \Theta(\beta - s) + \psi_{j \in A}^{(2)}(i\omega_n) e^{-i\omega_n s} \Theta(s - \beta) \right], \quad \omega_n = \frac{(2n+1)\pi}{\beta}, \quad (\text{S28})$$

$$\psi_{j \in B}(s) = \frac{1}{\sqrt{2\beta}} \sum_n \psi_{j \in B}(i\Omega_n) e^{-i\Omega_n s}, \quad \Omega_n = \frac{(2n+1)\pi}{2\beta}. \quad (\text{S29})$$

At the interface of regions A and B , the fields on the two sides are glued together by the twist operator σ , defined by

$$\sigma(i\omega_m^{(a)}, i\Omega_n) = \int_{(a-1)\beta}^{a\beta} \frac{d\tau}{\sqrt{2\beta}} e^{i[\omega_m^{(a)} - \Omega_n]\tau}, \quad a = 1, 2, \quad (\text{S30})$$

so that $\sigma(i\omega_m^{(a)}, i\Omega_n)$ is the overlap between the modes $\psi_{j \in A}^{(a)}(i\omega_m)$ and $\psi_{j \in B}(i\Omega_n)$. To prepare for the derivation of the replica action and the corresponding Green's functions, we also define the diagonal matrices of Matsubara frequencies $\omega := (\bigoplus_n \omega_n) \otimes \mathbf{1}_2$, $\Omega := \bigoplus_n \Omega_n$.

B. Saddle-point solution to the replica action

Consider the generic partition on the 1+1D chain, as depicted in Fig. S2 [Fig. 3(a) in main text]. We compute the entanglement entropy between regions A and B .

We again introduce the bilocal fields $G_{(2)}$ and $\Sigma_{(2)}$ at the SYK site, and then integrate out the free Majorana fields on the rest of the chain. The action becomes

$$-\frac{I_{(2)}}{N} = \frac{1}{2} \log \det \mathcal{M} - \frac{1}{2} \int ds_1 ds_2 G_{(2)}(s_1, s_2) \Sigma_{(2)}(s_1, s_2) + \frac{J^2}{4q} \int ds_1 ds_2 [2G_{(2)}(s_1, s_2)]^q, \quad (\text{S31})$$

Thus, $(A'_1)^{-1} = \mathbf{D}_{K_1, L_1}/t$. Similar results hold for $(A'_2)^{-1}$. Furthermore,

$$\det B_1 = t^{L_1} U_{L_1} \left(\frac{-i\Omega}{2t} \right), \quad (\text{S38})$$

$$\begin{aligned} \det A'_1 &= \det \left[A_1 - r_1^2 t \sigma R_{L_1} \left(\frac{-i\Omega}{2t} \right) \sigma^\dagger e_1 \right] \\ &= t^{K_1-1} U_{K_1-1} \left(\frac{-i\omega}{2t} \right) \det \left[-i\omega - t R_{K_1-1} \left(\frac{-i\omega}{2t} \right) - r_1^2 t \sigma R_{L_1} \left(\frac{-i\Omega}{2t} \right) \sigma^\dagger \right] \\ &= t^{K_1-1} U_{K_1-1} \left(\frac{-i\omega}{2t} \right) \det \left[t R_{K_1}^{-1} \left(\frac{-i\omega}{2t} \right) - r_1^2 t \sigma R_{L_1} \left(\frac{-i\Omega}{2t} \right) \sigma^\dagger \right]. \end{aligned} \quad (\text{S39})$$

Therefore,

$$\begin{aligned} -\frac{I_{(2)}}{N} &= \frac{1}{2} \log \det \left[-i\omega - \Sigma_{(2)} - q_1^2 t \mathbf{D}_{K_1, L_1} - q_2^2 t \mathbf{D}_{K_2, L_2} \right] \\ &\quad - \frac{1}{2} \int d\tau_1 d\tau_2 G(\tau_1, \tau_2) \Sigma_{(2)}(\tau_1, \tau_2) + \frac{J^2}{4q} \int d\tau_1 d\tau_2 [2G(\tau_1, \tau_2)]^q \\ &\quad + \frac{1}{2} \log \det \left[t R_{K_1}^{-1} \left(\frac{-i\omega}{2t} \right) - r_1^2 t \sigma R_{L_1} \left(\frac{-i\Omega}{2t} \right) \sigma^\dagger \right] + \frac{1}{2} \log \det \left[t R_{K_2}^{-1} \left(\frac{-i\omega}{2t} \right) - r_2^2 t \sigma R_{L_2} \left(\frac{-i\Omega}{2t} \right) \sigma^\dagger \right] \\ &\quad + \frac{1}{2} \log \det \left[t^{L_1+L_2+K_1+K_2-2} U_{L_1} \left(\frac{-i\Omega}{2t} \right) U_{L_2} \left(\frac{-i\Omega}{2t} \right) U_{K_1-1} \left(\frac{-i\omega}{2t} \right) U_{K_2-1} \left(\frac{-i\omega}{2t} \right) \right]. \end{aligned} \quad (\text{S40})$$

The saddle point equations is

$$G_{(2)}^{-1} = -i\omega - \Sigma_{(2)} - q_1^2 t \mathbf{D}_{K_1, L_1} - q_2^2 t \mathbf{D}_{K_2, L_2}. \quad (\text{S41})$$

On the other hand, the untwisted action on a single replica can be obtained by modifying Eq. (S12),

$$\begin{aligned} -\frac{I}{N} &= \frac{1}{2} \sum_n \log \left[-i\omega_n - \Sigma(\omega_n) - q_1^2 t D'_{K_1, L_1} \left(\frac{-i\omega_n}{2t} \right) - q_2^2 t D'_{K_2, L_2} \left(\frac{-i\omega_n}{2t} \right) \right] \\ &\quad - \frac{1}{2} \int d\tau_1 d\tau_2 G(\tau_1, \tau_2) \Sigma(\tau_1, \tau_2) + \frac{J^2}{4q} \int d\tau_1 d\tau_2 [2G(\tau_1, \tau_2)]^q \\ &\quad + \frac{1}{2} \sum_n \log \left[t R_{K_1}^{-1} \left(\frac{-i\omega_n}{2t} \right) - r_1^2 t R_{L_1} \left(\frac{-i\omega_n}{2t} \right) \right] + \frac{1}{2} \sum_n \log \left[t R_{K_2}^{-1} \left(\frac{-i\omega_n}{2t} \right) - r_2^2 t R_{L_2} \left(\frac{-i\omega_n}{2t} \right) \right] \\ &\quad + \frac{1}{2} \sum_n \log \left[t^{L_1+L_2+K_1+K_2-2} U_{L_1} \left(\frac{-i\omega_n}{2t} \right) U_{L_2} \left(\frac{-i\omega_n}{2t} \right) U_{K_1-1} \left(\frac{-i\omega_n}{2t} \right) U_{K_2-1} \left(\frac{-i\omega_n}{2t} \right) \right], \end{aligned} \quad (\text{S42})$$

where $D'_{K,L}$ has the same recursive structure as $\mathbf{D}_{K,L}$, with $D'_{0,L} \left(\frac{-i\omega_n}{2t} \right) = r^2 R_L \left(\frac{-i\omega_n}{2t} \right)$. Since all terms commute, it can be simplified into

$$D'_{K,L} \left(\frac{-i\omega_n}{2t} \right) := \frac{1 - R_{K-1} \left(\frac{-i\omega_n}{2t} \right) r^2 R_L \left(\frac{-i\omega_n}{2t} \right)}{R_{K-1}^{-1} \left(\frac{-i\omega_n}{2t} \right) - r^2 R_L \left(\frac{-i\omega_n}{2t} \right)}. \quad (\text{S43})$$

The second Rényi entropy is given by $S_2 = I_{(2)} - 2I$. We can further simplify the expression for the ground-state Rényi entropy by subtracting the zero S_2 when A and B are decoupled, thus dropping the last terms in (S40) and (S42). At $r = 0$, $\mathbf{D}_K = D'_K \left(\frac{-i\omega}{2t} \right) = R_K \left(\frac{-i\omega}{2t} \right)$. Denote the entropy terms in a decoupled system by \check{I} , and also let \check{G} be the Green's function G in (1) repeated on each replica, $\check{G} = G \otimes \mathbf{1}_2$, such that

$$\check{G}(\tau_1, \tau_2) = \begin{cases} G(\tau_1, \tau_2), & 0 \leq \tau_1, \tau_2 \leq \beta, \\ G(\tau_1 - \beta, \tau_2 - \beta), & \beta \leq \tau_1, \tau_2 \leq 2\beta, \\ 0, & \text{otherwise.} \end{cases} \quad (\text{S44})$$

Then, we arrive at the ground-state Rényi entropy

$$\begin{aligned} S_2/N &= [I_{(2)} - 2I - (\check{I}_{(2)} - 2\check{I})] / N \\ &= -\frac{1}{2} \log \det \left[G_{(2)}^{-1} \check{G} \right] + J^2 \left(\frac{1}{4q} - \frac{1}{4} \right) \int d\tau_1 d\tau_2 \{ [2\check{G}(\tau_1, \tau_2)]^q - [2G_{(2)}(\tau_1, \tau_2)]^q \} \\ &\quad + \frac{1}{2} \log \det \left[\frac{1 - r_1^2 R_{L_1} \left(\frac{-i\omega}{2t} \right) R_{K_1} \left(\frac{-i\omega}{2t} \right)}{1 - r_1^2 \sigma R_{L_1} \left(\frac{-i\Omega}{2t} \right) \sigma^\dagger R_{K_1} \left(\frac{-i\omega}{2t} \right)} \right] + \frac{1}{2} \log \det \left[\frac{1 - r_2^2 R_{L_2} \left(\frac{-i\omega}{2t} \right) R_{K_2} \left(\frac{-i\omega}{2t} \right)}{1 - r_2^2 \sigma R_{L_2} \left(\frac{-i\Omega}{2t} \right) \sigma^\dagger R_{K_2} \left(\frac{-i\omega}{2t} \right)} \right]. \end{aligned} \quad (\text{S45})$$

Note that with trivial modifications, the last line is simply the entanglement between two 1+1D Majorana lattice with (possibly different) uniform nearest-neighbor hoppings.

IV. DERIVATION OF TRANSMISSION AND REFLECTION IN THE SYK DEFECT CFT

A. Defect CFT

Here we derive the transmission and reflection coefficients for the SYK₂ defect CFT. We first carry out coarse graining to obtain a continuum theory with the SYK defect, and then calculate the transmission and reflection coefficient from the two-point function of the stress tensor across the defect. Consider the free Majorana chain,

$$H = i2t \sum_r \psi_r \psi_{r+1}, \quad \{\psi_r, \psi'_r\} = \delta_{ij}. \quad (\text{S46})$$

After a Fourier transformation, it is easy to see that the Fermi momenta are located at $k_F = 0$ and $k_F = \frac{\pi}{a}$, where a denotes the lattice constant. Then, we take the following identification between the lattice fermion and the continuum fermion field

$$\begin{cases} \psi_{2r} = \sqrt{\frac{a}{2}}[\psi_R(x_r) + \psi_L(x_r)], \\ \psi_{2r+1} = \sqrt{\frac{a}{2}}[\psi_R(x_r) - \psi_L(x_r)], \end{cases} \quad r \in \mathbb{Z}, \quad x_r \equiv 2ra. \quad (\text{S47})$$

Here, $\psi_{R,L}(x)$ is the continuum fermion field operator with $\{\psi_L(x), \psi_L(x')\} = \{\psi_R(x), \psi_R(x')\} = \delta(x - x')$, and $\{\psi_L(x), \psi_R(x')\} = 0$. Thus, the unit cell is effectively doubled with the two low-energy chiral modes folded to $k = 0$. Note also that $\psi_L^\dagger(x) = \psi_L(x)$ and $\psi_R^\dagger(x) = \psi_R(x)$.

In terms of the continuum field, with $v_F := at$, the Hamiltonian becomes

$$H = i \int dx v_F (\psi_R \partial_x \psi_R - \psi_L \partial_x \psi_L). \quad (\text{S48})$$

For N decoupled Majorana chains, we can duplicate the theory with an additional index $i = 1, \dots, N$. Then we are ready to add the SYK interaction to the theory. Without loss of generality, consider the SYK site to be the even site at 0,

$$\sum_{jl} i J_{jl} \delta_{r,0} \psi_{r,j}^\dagger \psi_{r,l} = \sum_{jl} i J_{jl} a \delta(x) [\psi_{j,R}(x) + \psi_{j,L}(x)] [\psi_{l,R}(x) + \psi_{l,L}(x)] = \sum_{jl} i 2a \delta(x) \tilde{J}_{jl} \Psi_j^\dagger(x) P \Psi_l(x), \quad (\text{S49})$$

where $\Psi = (\psi_L, \psi_R)^T$, $P = \frac{1}{2} \begin{pmatrix} 1 & 1 \\ 1 & 1 \end{pmatrix}$, $\delta(x) = \delta(2ra) = \delta_{r,0}/2a$, and we have introduced the dimensionless coupling $\tilde{J}_{jl} = a J_{ij}$. Recall that J_{ij} is a Gaussian random variable with mean zero and variance given by (S3).

Combined with the free part, it leads to the following continuum theory

$$\mathcal{L}_E = \sum_j \Psi_j^\dagger(x) (\partial_\tau - i v_F \partial_x \sigma^z) \Psi_j(x) + \sum_{jl} i \delta(x) \tilde{J}_{jl} \Psi_j^\dagger(x) P \Psi_l(x). \quad (\text{S50})$$

Denoting $G := \frac{1}{N} \sum_i \langle \Psi_i \Psi_i^\dagger \rangle$, the large- N equation of motion reads

$$\begin{aligned} G(x, x'; \omega) &= G_0(x, x'; \omega) + G_0(x, 0; \omega) \Sigma(\omega) G(0, x'; \omega), \\ \Sigma(\omega) &= 2\tilde{J}^2 P G(0, 0; \omega) P. \end{aligned} \quad (\text{S51})$$

where $\tilde{J} = Ja$ with J being the strength of the variance defined in (S3). In the following, we set $v_F = 1$ for simplicity; in other words, $a = 1/t$ and $\tilde{J} = J/t$. Notice that we have performed disorder average to derive the equation of motion. The equation of motion is presented in mixed coordinates because the spatial translation symmetry is broken by the defect, whereas the temporal one is respected. This large- N equation of motion can be solved straightforwardly, leading to the solution:

$$\begin{aligned} G(x, y; \omega) &= G_0(x, y; \omega) + \frac{i \operatorname{sgn}(\omega) (1 + \tilde{J}^2 - \sqrt{1 + 2\tilde{J}^2})}{4\tilde{J}^2} \\ &\quad \times \begin{pmatrix} [\operatorname{sgn}(x) + \operatorname{sgn}(\omega)][\operatorname{sgn}(y) - \operatorname{sgn}(\omega)] & -[\operatorname{sgn}(x) + \operatorname{sgn}(\omega)][\operatorname{sgn}(y) + \operatorname{sgn}(\omega)] \\ -[\operatorname{sgn}(x) - \operatorname{sgn}(\omega)][\operatorname{sgn}(y) - \operatorname{sgn}(\omega)] & [\operatorname{sgn}(x) - \operatorname{sgn}(\omega)][\operatorname{sgn}(y) + \operatorname{sgn}(\omega)] \end{pmatrix} e^{-(|x|+|y|)|\omega|} \end{aligned} \quad (\text{S52})$$

$$G_0(x, y; \omega) = i \left(\frac{\operatorname{sgn}(\omega)}{2} + \frac{\operatorname{sgn}(x-y)\sigma^z}{2} \right) e^{-|x-y||\omega|}, \quad (\text{S53})$$

which leads to the equal time correlation function

$$G(x, y) \equiv G(x, y; \tau = 0) = \frac{i\sigma^z}{x-y} + \frac{i(1 + \tilde{J}^2 - \sqrt{1 + 2\tilde{J}^2})}{2\tilde{J}^2(|x| + |y|)} \begin{pmatrix} -\operatorname{sgn}(x) + \operatorname{sgn}(y) & -\operatorname{sgn}(x) - \operatorname{sgn}(y) \\ \operatorname{sgn}(x) + \operatorname{sgn}(y) & \operatorname{sgn}(x) - \operatorname{sgn}(y) \end{pmatrix}. \quad (\text{S54})$$

The stress-energy tensor away from the defect is

$$T(x) = 2\psi^\dagger(x)P_R\partial_x\psi(x), \quad \bar{T} = -2\psi^\dagger(x)P_L\partial_x\psi(x), \quad (\text{S55})$$

where $P_L = \frac{1}{2}(1 + \sigma^z)$, and $P_R = \frac{1}{2}(1 - \sigma^z)$ are the projection to right and left movers, respectively. Using the full Green's function, the correlation function of stress-energy tensor is given by

$$\langle T(x)T(-x) \rangle = -4\text{Tr} \left[P_R G^{(1,0)}(x, -x) P_R G^{(1,0)}(x, -x) \right] = \frac{(1 - \sqrt{1 + 2\tilde{J}^2})^2}{4\tilde{J}^4(2x)^4}, \quad (\text{S56})$$

$$\langle \bar{T}(x)\bar{T}(-x) \rangle = -4\text{Tr} \left[P_L G^{(1,0)}(x, -x) P_L G^{(1,0)}(x, -x) \right] = \frac{(1 - \sqrt{1 + 2\tilde{J}^2})^2}{4\tilde{J}^4(2x)^4}, \quad (\text{S57})$$

$$\langle T(x)\bar{T}(x) \rangle = 4\text{Tr} \left[P_R G^{(1,0)}(x, x) P_L G^{(1,0)}(x, x) \right] = \frac{(1 + \tilde{J}^2 - \sqrt{1 + 2\tilde{J}^2})^2}{4\tilde{J}^4(2x)^4}, \quad (\text{S58})$$

$$\langle \bar{T}(-x)T(-x) \rangle = 4\text{Tr} \left[P_L G^{(1,0)}(-x, -x) P_L G^{(1,0)}(-x, -x) \right] = \frac{(1 + \tilde{J}^2 - \sqrt{1 + 2\tilde{J}^2})^2}{4\tilde{J}^4(2x)^4}, \quad (\text{S59})$$

in which $G^{(1,0)}(x, y) \equiv \partial_x G(x, y)$ and $G^{(0,1)}(x, y) \equiv \partial_y G(x, y)$. Hence, the transmission and reflection coefficients are [14]

$$\mathcal{T} = \frac{\langle T(x)T(-x) \rangle + \langle \bar{T}(x)\bar{T}(-x) \rangle}{\langle T(x)T(-x) \rangle + \langle \bar{T}(x)\bar{T}(-x) \rangle + \langle T(x)\bar{T}(x) \rangle + \langle \bar{T}(-x)T(-x) \rangle} = \frac{2}{3 + \tilde{J}^2 - \sqrt{1 + 2\tilde{J}^2}}, \quad (\text{S60})$$

$$\mathcal{R} = \frac{\langle T(x)\bar{T}(x) \rangle + \langle \bar{T}(-x)T(-x) \rangle}{\langle T(x)T(-x) \rangle + \langle \bar{T}(x)\bar{T}(-x) \rangle + \langle T(x)\bar{T}(x) \rangle + \langle \bar{T}(-x)T(-x) \rangle} = 1 - \frac{2}{3 + \tilde{J}^2 - \sqrt{1 + 2\tilde{J}^2}}, \quad (\text{S61})$$

leading to the transmission coefficient presented in the main text. Since the conformal solution is continuously connected to that of a free Ising CFT, it also reveals that our defect formally corresponds to the Dirichlet boundary condition in the Ising CFT. The defect state here is $|D, \phi\rangle$ with $\phi = \sin^{-1}(\sqrt{\mathcal{T}})/2$ [16, 53].

B. Lattice model

For completeness, we also derive the Green's function and transmission coefficient of the lattice model, which is infinite Majorana chains coupled at an SYK₂ site. The argument of the Green's function will follow the format $G(r, r', t; k, k', \omega)$ where the prime differentiates incoming and outgoing coordinates, and the semicolon separates spacetime and momentum-frequency coordinates, which are not present at the same time. The imaginary-time Dyson equation on the lattice reads

$$G(r, r'; i\omega_n) = G_0(r, r'; i\omega_n) + G_0(r, 0; i\omega_n)\Sigma(\omega_n)G(0, r'; i\omega_n), \quad (\text{S62})$$

Set the lattice constant $a = 1$. On a chain of length $L \rightarrow \infty$, we define the spatial Fourier transform

$$G(k, k') := \frac{1}{L} \sum_{r, r'} G(r, r') e^{-ikr + ik'r'}. \quad (\text{S63})$$

The free Green's function G_0 has the translational invariance $G_0(r, r') = G_0(r - r')$. Let

$$G_0(k) = \frac{1}{L} \sum_{\Delta r} G_0(\Delta r) e^{-ik\Delta r} = G_0(0; k) = G_0(0; k'). \quad (\text{S64})$$

Then, for $m \in \mathbb{Z}$

$$G_0(k, k') = 2\pi\delta(k - k' + 2m\pi)G_0(k). \quad (\text{S65})$$

Recall that

$$\begin{aligned} G_0(k, i\omega_n) &= \frac{1}{-i\omega_n - 2t \sin k}, \\ G_0(0, 0; i\omega_n) &= \frac{1}{\sqrt{-i\omega_n + 2t\sqrt{-i\omega_n - 2t}}} = \frac{1}{\sqrt{-\omega_n^2 - 4t^2}}. \end{aligned} \quad (\text{S66})$$

In addition, we can obtain $\Sigma(\omega_n)$ using Eq. (S19) and (S15),

$$\Sigma(\omega_n) = \frac{i}{2} \left[\sqrt{-\omega_n^2 - 4t^2} - \sqrt{-\omega_n^2 - 4t^2 - 8J^2} \right]. \quad (\text{S67})$$

Solving $G(0; k', i\omega_n) = G_0(0; k', i\omega_n) + G_0(0, 0; i\omega_n)\Sigma(\omega_n)G(0; k', i\omega_n)$ for $G(0; k', i\omega_n)$ gives

$$G(0, k'; i\omega_n) = \frac{1}{(-i\omega_n - 2t \sin k')} \frac{2}{2 - i + i\sqrt{1 + 8J^2/(\omega_n^2 + 4t^2)}}. \quad (\text{S68})$$

Solving $G(k, k', i\omega_n) = G_0(k, k', i\omega_n) + G_0(0; k, i\omega_n)\Sigma(\omega_n)G(0; k', i\omega_n)$ for $G(k, k', i\omega_n)$ gives

$$G(k, k', i\omega_n) = 2\pi\delta(k - k' + 2m\pi) \frac{1}{-i\omega_n - 2t \sin k} + \frac{1}{-i\omega_n - 2t \sin k} \sqrt{-\omega_n^2 - 4t^2} \frac{1 - \sqrt{1 + 8J^2/(\omega_n^2 + 4t^2)}}{\sqrt{1 + 8J^2/(\omega_n^2 + 4t^2)} - 1 - 2i} \frac{1}{-i\omega_n - 2t \sin k'}. \quad (\text{S69})$$

Note that G takes the standard form $G(z) = G_0(z) + G_0(z)\text{T}(z)G_0(z)$ with the second term containing the T-matrix. For real frequencies, one substitute $\omega_n^2 \rightarrow -\omega^2$. The initial and final scattering states are on shell with respect to the free Hamiltonian, conforming to Fermi's golden rule. When on shell, $\omega^2 - 4t^2 \rightarrow -4t^2 \cos^2 k$. Owing to energy conservation, at infinite time the surviving term is proportional to $\delta(2t \sin k - 2t \sin k') = [\delta(k - k' + 2m\pi) + \delta(k + k' - \pi + 2m\pi)]/|2t \cos k|$. Thus, for an incoming state of momentum k , the outgoing momentum is k and $\pi - k$. The amplitude of the $\sqrt{\omega^2 - 4t^2}$ factor also cancels the δ -function measure $|2t \cos k|$ when on shell. Finally, the reflection coefficient is simply given by $\left| \frac{1 - \sqrt{1 + 2 \sec^2(k) J^2 / t^2}}{\sqrt{1 + 2 \sec^2(k) J^2 / t^2} - 1 - 2i} \right|^2$.

Let $\tilde{J} = J/t$. The transmission and reflection coefficients are

$$\begin{aligned} \mathcal{T}(k) &:= |\langle k, t = \infty | k, t = -\infty \rangle|^2 = \frac{2}{3 + \tilde{J}^2 \sec^2 k - \sqrt{1 + 2\tilde{J}^2 \sec^2 k}}, \\ \mathcal{R}(k) &:= |\langle \pi - k, t = \infty | k, t = -\infty \rangle|^2 = 1 - \frac{2}{3 + \tilde{J}^2 \sec^2 k - \sqrt{1 + 2\tilde{J}^2 \sec^2 k}}. \end{aligned} \quad (\text{S70})$$

In the low-energy limit, $k \sim 0$. Then we recover the conformal result in Eq. (4) or (S60). Hence, there is a simple relation between the defect strengths in the continuum and on a lattice. These results may also be obtained by the LSZ formalism in the continuum limit [17].

V. DISCUSSIONS ON RÉNYI ENTROPY AND TRANSMISSION COEFFICIENT

A. Derivation of the transmission coefficient for energy defect in the Ising CFT

In this section, we briefly review the calculation of the transmission coefficient for an energy defect in the Ising CFT, i.e., the free Majorana model. We used a similar model as in the previous section to evaluate the transmission and reflection coefficient. In the presence of an energy defect, the continuum field theory reads

$$\mathcal{L}_E = \Psi^\dagger(x)(\partial_\tau - i\sigma^z \partial_x)\Psi(x) + g\delta(x)\Psi^\dagger(x)\sigma^y\Psi(x), \quad (\text{S71})$$

where g denotes the defect strength, and we set the Fermi velocity to be one for simplicity. Comparing this Lagrangian with the SYK defect (S50), the defect has a different form, and because the energy defect does not couple different flavors, we consider $N = 1$.

The scattering of the energy defect leads to the Schwinger-Dyson equation,

$$G(x_1, x_2; \omega) = G_0(x_1 - x_2; \omega) + G_0(x_1 - x_2; \omega)\Sigma(\omega)G_0(x_2; \omega) \quad (\text{S72})$$

$$\Sigma(\omega) = g \frac{\sigma^y}{1 - gG_0(0; \omega)\sigma^y}. \quad (\text{S73})$$

where $G = \langle \Psi\Psi^\dagger \rangle$ is the full propagator, and $G_0(x - y; \omega) = G_0(x, y; \omega)$ in (S53). Note that this Schwinger-Dyson equation is exact. The solution is

$$G(x_1, x_2, \tau_1, \tau_2) = \left(\begin{array}{cc} \frac{i[4+g^2-2g^2(\Theta(x_1)\Theta(-x_2)+\Theta(-x_1)\Theta(x_2))]}{2\pi(4+g^2)(x_{12}+i\tau_{12})} & \frac{i2g(\Theta(x_1)\Theta(x_2)-\Theta(-x_1)\Theta(-x_2))}{\pi(4+g^2)(x_1+x_2+i\tau_{12})} \\ -\frac{i2g(\Theta(x_1)\Theta(x_2)-\Theta(-x_1)\Theta(-x_2))}{\pi(4+g^2)(x_1+x_2+i\tau_{12})} & -\frac{i[4+g^2-2g^2(\Theta(x_1)\Theta(-x_2)+\Theta(-x_1)\Theta(x_2))]}{2\pi(4+g^2)(x_{12}+i\tau_{12})} \end{array} \right), \quad (\text{S74})$$

where $x_{12} := x_1 - x_2$ and $\tau_{12} := \tau_1 - \tau_2$

With the full propagator, we can evaluate the transmission and reflection coefficients via stress-energy tensors similar to the preceding section. The results are

$$\mathcal{T} = 1 - \frac{16g^2}{(4+g^2)^2}, \quad \mathcal{R} = \frac{16g^2}{(4+g^2)^2}. \quad (\text{S75})$$

This is consistent with Ref. 17.

In comparison, we note that the transmission and reflection coefficients in the bosonic counterpart is $\sqrt{\mathcal{T}} = 1 - \frac{ig}{4\omega+ig}$ and $\sqrt{\mathcal{R}} = \frac{-ig}{4\omega+ig}$ [17]. At low frequency, the defect is relevant, and accordingly $\mathcal{T} = 0$. This is discussed in detail later in Sec. VI A.

B. Relation between the effective central charge and the transmission coefficient

We discuss the relation between the transmission coefficient and the entanglement entropy. The entanglement entropy across the defect is given by an effective central charge \tilde{c}_n [45]

$$S_n = \frac{\tilde{c}_n(\mathcal{T})}{12} \left(1 + \frac{1}{n}\right) \log\left(\frac{L}{a}\right), \quad (\text{S76})$$

where S_n denotes Rényi- n entropy and a is the lattice constant. For von Neumann entropy, the effective central charge is [50]

$$\tilde{c}_1 = -\frac{6}{\pi^2} \{[(1+s)\log(1+s) + (1-s)\log(1-s)]\log s + (1+s)\text{Li}_2(-s) + (1-s)\text{Li}_2(s)\}, \quad s = \sqrt{\mathcal{T}}. \quad (\text{S77})$$

For the Rényi entropy, the results can be found in [52]. In particular, the Rényi-2 entropy calculated in our paper is

$$\tilde{c}_2(\mathcal{T}) = \frac{8}{\pi^2} \arcsin^2\left(\sqrt{\frac{\mathcal{T}}{2}}\right). \quad (\text{S78})$$

For the energy defect in the Majorana chain model, the transmission coefficient reads [50] $\sqrt{\mathcal{T}} = \frac{2}{1+g+1/(1+g)}$, where g is a parameter that captures the strength of the defect. In particular, for the Majorana chain model with a modified bond hopping studied in the main text, $g = (t' - t)/t$, with t (t') denoting the normal (defect) bond hopping strength. Note that the relation between the transmission coefficient derived from the continuum field theory (S75), and from the transfer matrix method is not straightforward. Nevertheless, they agree at the leading order as expected, since the continuum theory neglects higher-order contribution:

$$\mathcal{T} \approx 1 - g^2, \quad (\text{S79})$$

Therefore, the field theory calculation correctly predicts the leading behavior of the effective central charge

$$\tilde{c}_2 \approx \frac{1}{4\pi^2} - \frac{g^2}{2\pi^2}. \quad (\text{S80})$$

However, such a minimal consistency is violated for the SYK defect as discussed in the main text, as will be shown next.

C. Perturbative expansions for the SYK defect CFT

In the interface geometry where $L_1 = K_2 = 0$, the Rényi-2 entropy in (S45) or (7) in the main text simplifies to

$$S_2/N = \frac{1}{2} \text{Tr} \log[G_{(2)}\tilde{G}^{-1}] + J^2 \left(\frac{1}{4q} - \frac{1}{4}\right) \int d\tau_1 d\tau_2 \{[2\tilde{G}(\tau_1, \tau_2)]^q - [2G_{(2)}(\tau_1, \tau_2)]^q\}. \quad (\text{S81})$$

To leading order in J at $q = 2$,

$$\frac{1}{2} \text{Tr} \log[G_{(2)}\tilde{G}^{-1}] = -\frac{1}{2} \text{Tr} \log[G_{(2)}^{-1}\tilde{G}] + J^2 \left(\frac{1}{4q} - \frac{1}{4}\right) \int d\tau_1 d\tau_2 \{[2\tilde{G}(\tau_1, \tau_2)]^q - [2G_{(2)}(\tau_1, \tau_2)]^q\}. \quad (\text{S82})$$

Let $\Gamma_{(2)} \equiv G_{(2)}|_{J=0} = (-i\omega - t\mathbf{D}_{K_1, L_1} - t\mathbf{D}_{K_2, L_2})^{-1}$ and $\tilde{\Gamma} \equiv \tilde{G}|_{J=0} = (-i\omega - t\mathbf{D}'_{K_1, L_1} - t\mathbf{D}'_{K_2, L_2})^{-1}$. Then

$$\begin{aligned} \frac{1}{2} \text{Tr} \log [G_{(2)} \tilde{G}^{-1}] &= \frac{1}{2} \text{Tr} \log \left[\frac{-i\omega - 2J^2 \tilde{\Gamma} - t\mathbf{D}'_{K_1, L_1} - t\mathbf{D}'_{K_2, L_2}}{-i\omega - 2J^2 \Gamma_{(2)} - t\mathbf{D}_{K_1, L_1} - t\mathbf{D}_{K_2, L_2}} \right] \\ &= \frac{1}{2} \text{Tr} \log \left[\frac{-i\omega - 2J^2 \tilde{\Gamma} - tR_{K_1} \left(\frac{-i\omega}{2t} \right) - tR_{L_2} \left(\frac{-i\omega}{2t} \right)}{-i\omega - 2J^2 \Gamma_{(2)} - tR_{K_1} \left(\frac{-i\omega}{2t} \right) - t\sigma R_{L_2} \left(\frac{-i\omega}{2t} \right) \sigma^\dagger} \right] \end{aligned} \quad (\text{S83})$$

$$\begin{aligned} &= \frac{1}{2} \text{Tr} \log [G_{(2)} \tilde{G}^{-1} (1 + 2J^2 \Gamma_{(2)} G_{(2)} - 2J^2 \tilde{\Gamma} \tilde{G})] + O(J^4) \\ &= \frac{1}{2} \text{Tr} \log [\tilde{\Gamma}^{-1} \Gamma_{(2)}] + J^2 \text{Tr} [\Gamma_{(2)}^2 - \tilde{\Gamma}^2] + O(J^4). \end{aligned} \quad (\text{S84})$$

For the integral,

$$-\frac{3J^2}{4} \int d\tau_1 d\tau_2 \{[\tilde{G}(\tau_1, \tau_2)]^2 - [G_{(2)}(\tau_1, \tau_2)]^2\} = -\frac{3J^2}{4} \int d\tau_1 d\tau_2 \{[\tilde{\Gamma}(\tau_1, \tau_2)]^2 - [\Gamma_{(2)}(\tau_1, \tau_2)]^2\}. \quad (\text{S85})$$

Due to fermionicity, $\Gamma(\tau_1, \tau_2) = -\Gamma(\tau_2, \tau_1)$. Then $\text{Tr}(\Gamma^2) \equiv \int d\tau_1 d\tau_2 \Gamma(\tau_1, \tau_2) \Gamma(\tau_2, \tau_1) = -\int d\tau_1 d\tau_2 \Gamma(\tau_1, \tau_2)^2$. Thus,

$$\frac{S_2}{N} = \frac{S_2}{N} \Big|_{J=0} + \frac{J^2}{4} \int d\tau_1 d\tau_2 \{[\tilde{\Gamma}(\tau_1, \tau_2)]^2 - [\Gamma_{(2)}(\tau_1, \tau_2)]^2\} + O(J^4). \quad (\text{S86})$$

Therefore, the leading order change in S_2 and hence \tilde{c}_2 is J^2 . However, from Eq. (S60) or (4) in the main text, $\mathcal{T} = 2/(3 + \tilde{J}^2 - \sqrt{1 + 2\tilde{J}^2}) \approx 1 - J^4/2$. Consequently, the leading-order change in $\tilde{c}_2(\mathcal{T})$ is J^4 , in disagreement with that extracted from the scaling of S_2 , as plotted in Fig. 4(d) in the main text.

Finally, we address the independence of the g -function on J in the thermodynamic limit. In the setup to compute the g -function, $K_1 = K_2 = K$ and $L_1 = L_2 = L$. When K is large, $\lim_{K \rightarrow \infty} \mathbf{D}_{K, L} = \lim_{K \rightarrow \infty} D'_{K, L} \left(\frac{-i\omega}{2t} \right) = \lim_{K \rightarrow \infty} R_{K+L} \left(\frac{-i\omega}{2t} \right)$ for low-frequency components. In this case, the defect is too far from the interface to affect each other. Thus, $G_{(2)} \approx \tilde{G}$. As a result, S_2 comes only from noninteracting chains. In contrast, when the defect is next to the interface, e.g., $K_2 = 0$ as in (S83), the twist operator is immediately present in $G_{(2)}$, so its effect survives in the thermodynamic limit.

VI. FURTHER APPLICATIONS

In this section, we discuss further application of our saddle-point numerical functional determinant method.

A. Bosonic SYK defect

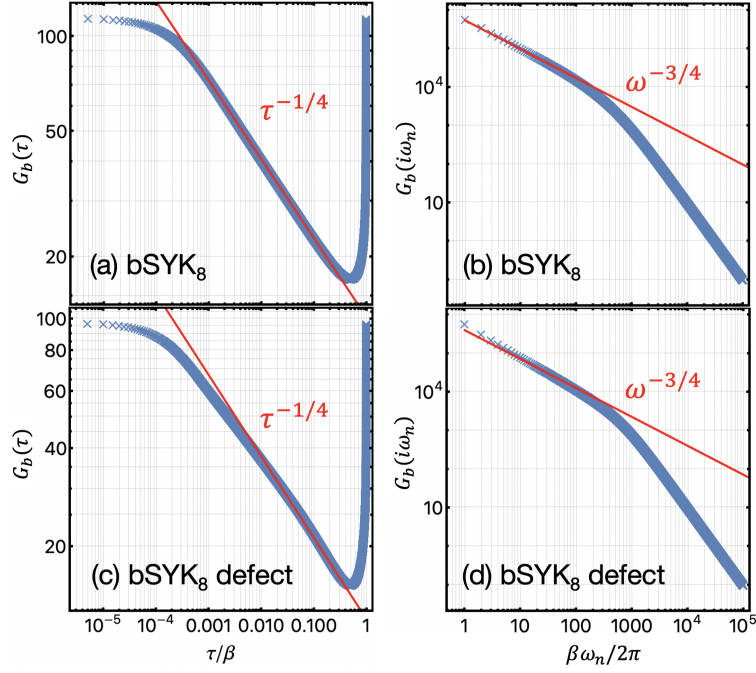
Our method can be easily extended to other defect theories. An example is the Yukawa-SYK defect coupling N free majorana channels and M free boson channels at the defect site [104]. Another example is N bosonic channels coupled at a bosonic SYK (bSYK) defect. We showcase the bSYK defect model below, and leave the study of the Yukawa-SYK defect for future work [105].

Consider the bosonic counterpart to our model. The action reads

$$-I = -\frac{1}{2} \sum_{j,r} \int d\tau [(\partial_\tau \varphi_{j,r})^2 - 2t\varphi_{j,r}\varphi_{j,r+1} + 2t\varphi_{j,r}^2] + \int d\tau \sum_{j_1, \dots, j_q} J_{j_1, \dots, j_q} \varphi_{j_1, 0} \dots \varphi_{j_q, 0}. \quad (\text{S87})$$

The chain index is $j = 1, \dots, N$. To the left of the defect are L sites, and to the right K sites. In the large N limit, assuming time translational invariance, the Schwinger-Dyson equations in imaginary time τ and Matsubara frequencies $\omega_n = 2\pi n/\beta$ reads

$$\begin{aligned} G_b(i\omega_n) &= \left[\omega_n^2 + 2t - tR_L \left(\frac{\omega_n^2}{2t} + 1 \right) - tR_K \left(\frac{\omega_n^2}{2t} + 1 \right) - \Sigma_b(i\omega_n) \right]^{-1}, \\ \Sigma_b(\tau_1, \tau_2) &= J^2 G_b(\tau_1, \tau_2)^{q-1}. \end{aligned} \quad (\text{S88})$$



Supplementary Figure S3. Green's function in imaginary time and Matsubara frequency of (a)–(b) the bosonic SYK₈ model, and (c)–(d) the bosonic SYK₈ defect coupled to a large N number of chains (S88). Red lines show the corresponding power laws of the conformal solution (S91). The parameters are $J/t = 1$, $\beta J = 2000$.

For $t = 0$ we recover the self-consistence equations for the bSYK. Albeit its unstable nature, one can solve the IR equations formally,

$$G_b^c(i\omega) = -1/\Sigma_b^c(i\omega), \quad \Sigma_b^c(\tau) = J^2 G_b^c(\tau)^{q-1}, \quad (\text{S89})$$

for a conformal solution G_b^c when $q \neq 2$ [101],

$$\begin{aligned} G_b^c(\tau) &= \left[\left(\frac{1}{2} - \frac{1}{q} \right) \frac{\cot(\pi/q)}{\pi J^2} \right]^{1/q} |\tau|^{-2/q}, \\ \Sigma_b^c(i\omega) &= \left[\left(\frac{1}{2} - \frac{1}{q} \right) \frac{\cot(\pi/q)}{\pi J^2} \right]^{-1/q} \frac{|\omega|^{1-2/q}}{2 \sin(\pi/q) \Gamma(1-2/q)}. \end{aligned} \quad (\text{S90})$$

At finite temperatures,

$$\begin{aligned} G_b^c(\tau) &= \left[\left(\frac{1}{2} - \frac{1}{q} \right) \frac{\pi \cot(\pi/q)}{\beta^2 J^2} \right]^{1/q} \left| \sin \left(\frac{\pi \tau}{\beta} \right) \right|^{-2/q}, \\ \Sigma_b^c(i\omega_n) &= \frac{\beta J^{2/q}}{\pi} \left[\frac{\beta^2 \tan(\pi/q)}{2\pi} \frac{1-2/q}{1-2/q} \right]^{-1+1/q} \sin \left(\frac{\pi}{q} \right) \text{B} \left(\frac{2}{q} - 1, n + 1 - \frac{1}{q} \right), \end{aligned} \quad (\text{S91})$$

where $\text{B}(x, y) := \Gamma(x)\Gamma(y)/\Gamma(x+y)$ is the beta function. Since the engineering dimension $[\varphi(x, \tau)] = 0$, the SYK interaction is relevant for all q 's. Consequently, the conformal solutions above hold at IR for the defect as well. However, since the solution is unstable, some pinning is required to converge to this solution. Below, we outline the intricacies in the numerics.

We discretize the imaginary time into $\delta\tau$, and truncate the Matsubara frequency, i.e., $-\beta/2\delta\tau < n \leq \beta/2\delta\tau$, so that the time and frequency grids are the same size. Since bSYK itself is unstable [84, 101], we enforce both time translational invariance and particle-hole symmetry, i.e., $G_b(\tau_1, \tau_2) = G_b(\tau_1 - \tau_2)$, and $G_b(\tau_1 - \tau_2) = G_b(\tau_2 - \tau_1)$. Furthermore, we pin the zero frequency term of G_b^{-1} to the conformal solution [103], and instead iterate with $G_b'^{-1}(i\omega_n) := G_b^{-1}(i\omega_n) + \Sigma_b(0) - \Sigma_b^c(0) - \Sigma_b(i\omega_n)$. The result is shown in Fig. S3. It is clear that the SYK term dominates IR physics. Note that although the power law agrees with the conformal solutions, the exact values are not identical. In particular, for the converged solution $\Sigma_b(0) \neq \Sigma_b^c(0)$.

In the bosonic case, the transmission is completely cut off for the SYK defect, as it is for a mass defect. Both can be solved in the LSZ formalism. Recall that the impurity T -matrix satisfy a Dyson series made up of the bare local Green's function

$g_0(\omega + i\eta) := G_0(x = y = 0, \omega + i\eta)$, and the bare self-energy at the impurity site Σ_0 [17],

$$T(\omega + i\eta) = \frac{1}{\Sigma_0^{-1}(\omega + i\eta) - g_0(\omega + i\eta)}. \quad (\text{S92})$$

In the case of a mass defect of the form $\int d\tau dx J^2 \phi^2(x) \delta(x)$, the bare self-energy $\Sigma_0(\omega + i\eta) = iJ^2$. The reflection coefficient can be obtained from the LSZ approach following Ref. 17, using $\mathcal{R} = |T/2p|^2$ where p is the momentum of the on-shell boson. It further simplifies to $\mathcal{R} = |T/2\omega|^2$ in our massless case. For the 1+1D real boson, $g_0(\omega + i\eta) = 1/\sqrt{(\omega + i\eta)^2}$. The result for the mass defect is

$$\mathcal{R} = \left| \frac{iJ^2}{2\omega - iJ^2} \right|^2 \xrightarrow{\omega \rightarrow 0} 1. \quad (\text{S93})$$

This also follows from the classic solution to a delta potential scattering in 1D [100]. As for the bSYK defect, let $\sigma(\tau) = g_0(\tau)^{q-1}$, then $\Sigma_0(\omega + i\eta) = iJ^2\sigma(\omega + i\eta)$. Thus, one can substitute $J^2 \rightarrow J^2\sigma(\omega + i\eta)$ in (S93) above. Since $[\phi(x, \tau)] = 0$, $[\sigma(\tau)] = 0$, and $[\sigma(\omega + i\eta)] = -1$. Therefore, in the limit $\omega \rightarrow 0$, one can see that $\mathcal{R} = J^4/[J^2 + O(\omega^2)]^2 \rightarrow 1$, without explicit calculations.

B. Interacting bulk CFT

Here we discuss how to extend our saddle-point method in the presence of onsite self-energy to accommodate interacting CFTs in the bulk. A concrete example is the SYK lattice in 1+1D at large N , with a defect site indexed 0. Once again we introduce the conjugate-pair fields (G_r, Σ_r) , but now on each site r . Thus, G_j becomes the local Green's function, i.e., $G_r(\tau_1, \tau_2) \sim \psi_r(\tau_1)\psi_r(\tau_2)/N$, and Σ_r becomes the self-energy on site r . The part of the action containing the original field ψ assumes the form

$$-I[\psi] = -\frac{1}{2} \sum_{j,r,r'} \int d\tau_1 d\tau_2 \psi_{j,r}(\tau_1) [(\partial_{\tau_1} \delta_{r,r'} - i h_{r,r'}) \delta(\tau_1 - \tau_2) - \Sigma_r(\tau_1, \tau_2) \delta_{r,r'}] \psi_{j,r'}(\tau_2), \quad (\text{S94})$$

where h is the hopping matrix. Denote $A = (\partial_{\tau_1} \delta_{r,r'} - i h_{r,r'}) \delta(\tau_1 - \tau_2) - \Sigma_r(\tau_1, \tau_2) \delta_{r,r'}$. This leads to as many saddle-point equations as the length of the lattice. Denote the minor of A with respect to entries i, j by $[A]_{ij}$, the saddle-point equations are

$$\begin{aligned} G_r(i\omega_n) &= \det[A]_{rr}(i\omega_n) / \det A(i\omega_n), \\ \Sigma_r &= \Sigma_r[G_r]. \end{aligned} \quad (\text{S95})$$

The self-energy Σ_r is a function of G_r , same as before. Therefore, naively one needs to solve $2L$ coupled self-consistency equations, which limits the system size accessible.

A reduction in the finite-size effect can be achieved if the left and right ends of the system are coupled to chains of infinite length, acting as baths. They are assumed to have a translationally invariant self-energy. Then, the function determinant including both the defect region (d) and the baths to the left (L) and right (R) is given by

$$\frac{1}{2} \log(\det A_L \det A_d \det A_R), \quad (\text{S96})$$

in which

$$A_{L/R} = -i\omega - \Sigma_{L/R} - \frac{t^2}{-i\omega - A_{L/R}}, \quad (\text{S97})$$

$$A_d = A - \frac{t^2}{-i\omega - A_L} - \frac{t^2}{-i\omega - A_R}. \quad (\text{S98})$$

Here, the chains are taken to be infinite as follows. A general iteration equation at the n -th left (or right) most site is

$$A_n = -i\omega - \Sigma_n - \frac{t^2}{-i\omega - A_{n-1}}, \quad A_1 = -i\omega - \Sigma_1. \quad (\text{S99})$$

Assuming a translationally invariant Σ_n and taking $n \rightarrow \infty$ gives the above equation for $A_{L/R}$. With (S97),

$$A_{L/R} = -i\omega - \frac{1}{2} \left(\Sigma_{L/R} + \text{sgn}(\omega) \sqrt{4t^2 + \Sigma_{L/R}^2} \right) \quad (\text{S100})$$

The Dyson equation in the frequency space is

$$G_{L/R} = - \left[A_{L/R}^{-1} + A_d^{-1} \left(\frac{t}{-i\omega - A_{L/R}} \right)^2 \right] \frac{\partial A_{L/R}}{\partial \Sigma_{L/R}}, \quad G_d = A_d^{-1}, \quad (\text{S101})$$

$$\frac{\partial A_{L/R}}{\partial \Sigma_{L/R}} = -\frac{1}{2} \left(1 + \frac{\text{sgn}(\omega) \Sigma_{L/R}}{\sqrt{4t^2 + \Sigma_{L/R}^2}} \right). \quad (\text{S102})$$

The self-energies are again a function of the respective local Green's functions.

C. Periodic boundary condition

We provide a simple example to illustrate how our method can be extended to the periodic boundary condition. Let the system be divided into A , B , and C blocks, the sizes of which are $K \times K$, $L \times L$, and $M \times M$, respectively. The defect is located in B . Define a shorthand for the special matrices $(e_{mn})_{ij} := \delta_{i,m} \delta_{n,j}$. On a periodic boundary condition with short-range hoppings t , the functional determinant takes the form

$$\begin{aligned} \det \left(\begin{array}{c|cc} A & & t \\ \hline t & B & t^\dagger \\ \hline t^\dagger & & C \end{array} \right) &= \det A \det \left(\begin{array}{c|c} B - e_{11} t A_{KK}^{-1} t^\dagger & t A_{K1}^{-1} t \\ \hline t^\dagger A_{1K}^{-1} t^\dagger & C - e_{MM} t^\dagger A_{11}^{-1} t \end{array} \right) \\ &= \det A \det(C - e_{MM} t^\dagger A_{11}^{-1} t) \times \det \left[B - e_{11} t^\dagger A_{KK}^{-1} t - e_{KK} t A_{K1}^{-1} t (C - e_{MM} t^\dagger A_{11}^{-1} t)^{-1} t^\dagger A_{1K}^{-1} t^\dagger \right. \\ &\quad \left. - e_{1L} t A_{K1}^{-1} t (C - e_{MM} t^\dagger A_{11}^{-1} t)^{-1} t - e_{L1} t^\dagger (C - e_{MM} t^\dagger A_{11}^{-1} t)^{-1} t^\dagger A_{1K}^{-1} t^\dagger - e_{LL} t^\dagger (C - e_{MM} t^\dagger A_{11}^{-1} t)^{-1} t^\dagger \right]. \quad (\text{S103}) \end{aligned}$$

The last determinant can be easily computed if B is a defect or a small region. In general, one will encounter the determinant of matrices of the following kind,

$$A_1(h_1; \omega_1; \omega_2 \dots \omega_n - 1; \omega_n) := \begin{pmatrix} \omega_1 & t^\dagger & & h \\ t & \omega_2 & \ddots & \\ & \ddots & \ddots & \ddots \\ & & \ddots & \ddots & t^\dagger \\ h^\dagger & & & t & \omega_n \end{pmatrix}. \quad (\text{S104})$$

The determinant of A_1 can be computed recursively:

$$\begin{aligned} \det A_1(h_1; \omega_1; \omega_2 \dots \omega_{n-1}; \omega_n) &= \omega_1 \det A_2(t\omega_1^{-1}h_1; \omega_2 - t\omega_1^{-1}t^\dagger; \omega_3 \dots \omega_{n-1}; \omega_n - h_1^\dagger \omega_1^{-1}h_1), \\ \det A_{m-1}(h; \nu; \omega_m \dots \omega_{n-1}; \lambda) &= \nu \det A_m(t\nu^{-1}h; \omega_m - t\nu^{-1}t^\dagger; \omega_{m+1} \dots \omega_{n-1}; \lambda - h^\dagger \nu^{-1}h). \quad (\text{S105}) \end{aligned}$$

The process continues until A_{n-2} , when the matrix dimension is reduced to 3. This has the same order of complexity as Eq. (S37).